NASA Technical Paper 1717

Development and Test Results of a Flight Management Algorithm for Fuel-Conservative Descents in a Time-Based Metered Traffic Environment

Charles E. Knox
Langley Research Center
Hampton, Virginia

Dennis G. Cannon
Boeing Commercial Airplane Company
Seattle, Washington

National Aeronautics
and Space Administration

**Scientific and Technical
Information Branch**

1980

A

SUMMARY

The Federal Aviation Administration has developed an automated time-based metering form of air traffic control for arrivals into the terminal area called local flow management/profile descent (LFM/PD). The LFM/PD concept provides fuel savings by matching the airplane arrival flow to the airport acceptance rate through time control computations and by allowing the pilot to descend at his discretion from cruise altitude to the metering fix in an idle-thrust, clean configuration (landing gear up, flaps zero, and speed brakes retracted). Substantial fuel savings have resulted from LPM/PD but air traffic control workload is high since the radar controller maintains time management for each airplane through either speed control or path stretching with radar vectors. Pilot workload is also high since the pilot must plan for an idle-thrust descent to the metering fix using various rules of thumb.

The National Aeronautics and Space Administration (NASA) has flight-tested a flight management descent alogrithm designed to improve the accuracy of delivering an airplane to a metering fix at a time designated by air traffic control in its Terminal Configured Vehicle (TCV) Boeing 737 research airplane. This alogrithm provides a three-dimensional path with terminal time constraints (four-dimensional) for an airplane to make an idle-thrust, clean-configured descent to arrive at the metering fix at a predetermined time, altitude, and airspeed. The descent path is calculated for a constant Mach/airspeed schedule by using linear approximations of airplane performance accounting for gross weight, wind, and nonstandard pressure and temperature effects.

Flight test data were obtained on 19 flight test runs to the metering fix. The standard deviation of metering fix arrival time error was 12 seconds with no arrival time error greater than 29 seconds. Comparable statistics for time error accumulated between the top of descent and the metering fix (approximately 40 n. mi.) are a 6.9-second standard deviation with no error greater than 15 seconds. The calibrated airspeed and altitude errors at the metering fix have standard deviations of 6.5 knots and 23.7 m (77.8 ft), respectively, and the maximum errors were less than 12.9 knots and 51.5 m (169 ft).

INTRODUCTION

Rising fuel costs combined with other economic pressures have resulted in industry requirements for more efficient air traffic control and aircraft operations. The Federal Aviation Administration (FAA) has developed an automated form of air traffic control (ATC) for arrivals into the airport terminal area. This concept is called local flow management/profile descent (LFM/PD) and provides for increased airport capacity and fuel savings by combining time-based metering with profile descent procedures. Time-based metering procedures provide for sequencing arrivals to the airport through time control of airplanes at metering fixes located 30 to 40 n. mi. from the airport. Time metering the airplanes at these fixes reduces the low altitude vectoring (and associated

fuel consumption) required to position the airplanes into a final queue for landing. In addition, delays due to terminal area sequencing may be absorbed at higher altitudes further minimizing fuel usage (refs. 1 and 2).

Profile descent procedures permit the initiation of the airplane descent at the pilot's discretion so that the airplane passes the metering fix at a specified altitude and airspeed. This procedure allows the pilot to plan the descent in a fuel-conservative manner accounting for the performance characteristics of his particular airplane.

In the original operational concept of the time-based metering LFM/PD program, the flight crew was responsible for both the descent and time navigation to the metering fix. However, the pilots had little or no computed guidance to aid them with this highly constrained (fuel-conservative descent with a fixed time objective), four-dimensional (4-D) navigation problem. Flight crews were forced to rely on past experience and various rules of thumb to plan descents. This practice resulted in unacceptably high cockpit workloads and the full potential of fuel savings from a planned descent not being obtained (ref. 3).

In an effort to reduce the cockpit workload, the responsibility of delivering the airplane to the metering fix at an assigned time was transferred to the ATC controller. The ATC controller directs the pilots with path stretching radar vectors and/or speed control commands as required so that each airplane crosses the metering fix at its assigned time. These operations have resulted in airplane arrival time accuracy at the metering fix of between 1 and 2 minutes (ref. 4). Improved arrival time accuracy and resulting increased fuel savings could be obtained at the cost of a significant increase in the ATC controller's workload.

Splitting the navigation responsibilities between the flight crew and ATC controller reduced the pilot's workload. However, when the ATC controller must apply path stretching or speed control for time management purposes, the pilot is forced to deviate from his planned descent profile; thus, more than the minimum fuel required is used.

The NASA has flight-tested in its Terminal Configured Vehicle (TCV) Boeing 737 research airplane a flight management descent alogrithm designed to increase fuel savings by reducing the time dispersion of airplanes crossing the metering fix at an ATC-designated time by transferring the responsibility of time navigation from the radar controller to the flight crew. The alogrithm computes a profile descent from cruise altitude to the metering fix based on airplane performance at idle thrust and in a clean configuration (landing gear up, flaps zero, and speed brakes retracted). Time and path guidance are provided to the pilot for a constant Mach descent followed by a constant airspeed descent to arrive at the metering fix at a predetermined (ATC specified) time, altitude, and airspeed.

Flight tests using the flight management descent algorithm were conducted in the Denver, Colorado, LFM/PD ATC environment. The purpose of these flight tests was to quantify the accuracy of the descent algorithm and to investigate the compatibility and pilot acceptability of an airplane equipped with a

4-D area navigation system in an actual ATC environment. This report describes the flight management descent algorithm and presents the results of these tests.

Use of company names or designations in this report does not constitute an official endorsement of such companies or products, either expressed or implied, by the National Aeronautics and Space Administration.

SYMBOLS AND ABBREVIATIONS

ACLT	actual computed landing time
ARTCC	air route traffic control center
ATC	air traffic control
a	temperature lapse rate, K/m
BARO	barometric altimeter setting, mb
CAS	calibrated airspeed, knots
CAS_d	calibrated airspeed used during descent, knots
$CAS_{d,i}$	computed initial descent calibratred airspeed, knots
$CAS_{d,max}$	maximum operational descent calibrated airspeed, knots
$CAS_{d,min}$	minimum operational descent calibrated airspeed, knots
CRT	cathode-ray tube
$D_{w,c}$	magnetic wind direction measured at cruise altitude, deg
$D_{w,grd}$	magnetic wind direction at airport, deg
$(D_w)_h$	magnetic wind direction evaluated at altitude h, deg
$\left(\frac{dD_w}{dh}\right)_H$	wind direction gradient with respect to altitude for high altitude segment, deg/m
$\left(\frac{dD_w}{dh}\right)_L$	wind direction gradient with respect to altitude for low altitude segment, deg/m
$\left(\frac{\dot{dh}}{dh}\right)_{M_d}$	change in altitude rate with respect to change in altitude evaluated at Mach number M_d, sec^{-1}

$\left(\frac{dS_w}{dh}\right)_H$ wind speed gradient with respect to altitude for high altitude segment, knots/m

$\left(\frac{dS_w}{dh}\right)_L$ wind speed gradient with respect to altitude for low altitude segment, knots/m

EADI electronic attitude director indicator

EHSI electronic horizontal situation indicator

ETA estimated time of arrival

FLnnn flight level

GW gross weight, N

h altitude, m

h_{AP} altitude at aim point, m

h_c altitude at cruise, m

h_{GP} geopotential altitude, m

h_{grd} airport elevation, m

h_I indicated altitude, m

h_{MF} altitude at metering fix, m

h_p pressure altitude, m

h_p' pressure altitude evaluated with nonstandard sea-level temperature, m

h_{XO} altitude to transition from constant Mach descent to constant airspeed descent, m

$\dot{h}$ altitude rate, m/sec

$(\dot{h})_{CAS_d}$ altitude rate evaluated at calibrated airspeed CAS_d, m/sec

$(\dot{h})_h$ altitude rate evaluated at altitude h, m/sec

$(\dot{h})_{M_d}$ altitude rate evaluated at Mach number M_d, m/sec

$K_{\dot{h}}$ gross weight multiplication factor for altitude rate for constant calibrated airspeed descent

$K_{\dot{dh}/dh}$	gross weight multiplication factor for change of altitude rate with respect to change of altitude for constant Mach descent
K_1	$= \left(\frac{\dot{dh}}{dh}\right)_{M_d}$, corrected for gross weight effects, (m/sec)/m
K_2	equation constant, m/sec
LFM/PD	local flow management/profile descent
l_{AP}	distance between metering fix and aim point, n. mi.
l_t	distance between entry fix and metering fix, n. mi.
M	Mach number
M_c	Mach number at cruise
M_d	Mach number in descent
$M_{d,i}$	computed initial descent Mach number
$M_{d,max}$	maximum operational descent Mach number
$M_{d,min}$	minimum operational descent Mach number
NCDU	navigation control and display unit
NCU	navigation computer unit
p_o	standard atmospheric pressure at sea level, N/m^2
p_{st}	static pressure, N/m^2
R	gas constant, m/K
RNAV	area navigation
$S_{w,c}$	wind speed measured at cruise altitude, knots
$S_{w,grd}$	wind speed at airport, knots
$(S_w)_h$	wind speed evaluated at altitude h, knots
TAS	true airspeed, knots
TCV	Terminal Configured Vehicle
TRK	airplane magnetic track angle along ground, deg
T_o	standard sea-level temperature, K

T_o'	nonstandard sea-level temperature, K
T_{st}	static temperature, K
t	time, sec
t_E	time error for descent speed convergence criteria, sec
t_{EF}	time assigned to cross entry fix, hr:min:sec
t_{MF}	time assigned to cross metering fix, hr:min:sec
VORTAC	very high frequency omnidirectional range and distance measuring equipment
$(W_H)_h$	head-wind component along airplane ground track evaluated at altitude h, knots
$\ddot{x}$	acceleration, knots/sec
$\ddot{x}_c$	acceleration at cruise altitude (idle thrust, clean configuration), knots/sec
ΔCAS	calibrated airspeed increment or decrement, knots
Δh_p	altitude bias correction for nonstandard atmospheric pressure, m
Δh_T	altitude error due to nonstandard temperature effects, m
Δl_j	length of path segment j, n. mi.
ΔM	Mach number increment or decrement
Δt_j	time required to fly on path segment j, sec
Δt_{max}	maximum time to fly between entry fix and metering fix (flown at minimum operational speeds), sec
Δt_{min}	minimum time to fly between entry fix and metering fix (flown at maximum operational speeds), sec
Δt_{req}	time required to fly between entry fix and metering fix, sec

ARTCC AUTOMATED LOCAL FLOW MANAGEMENT/PROFILE DESCENT DESCRIPTION

The ATC concept of automated local flow management/profile descents utilizing time-based metering is designed to permit operators of high-performance, turbine-powered airplanes to descend in a clean configuration at idle thrust to a point within the airport terminal area. Significant fuel savings are achieved on a fleet-wide (all users) basis by matching the airplane arrival

rate into the terminal area to the airport's arrival acceptance rate which reduces the need for holding and low altitude vectoring for sequencing. Fuel savings are also achieved on an individual airplane basis by permitting the pilot to descend in a fuel efficient manner at his discretion. In addition to arrival fuel savings, safety, noise abatement, and standardization of arrival procedures are all enhanced (ref. 5).

The Denver ARTCC's automated version of LFM/PD employs four metering fixes located around the Stapleton International Airport. Each arriving high-performance airplane is time-based metered to one of these four metering fixes. Metering is accomplished by using the ARTCC computer with consideration given to the following parameters:

(1) Airport acceptance rate (number of arrivals per unit time) specified by the Stapleton International Airport tower personnel

(2) Nominal path and airspeed profiles associated with each of the four metering fixes to the runway

(3) True airspeed filed on the airplane's flight plan

(4) Airplane position detected by ATC radar

(5) Forecast winds-aloft data from several stations in the Denver ARTCC area and/or measured winds from pilot reports

These parameters are processed by the ARTCC computer to determine an estimated time of arrival that each metered airplane would land on the runway, assuming no conflicts. The ETA's for all metered airplanes are chronologically ordered and compared to determine whether any of the airplanes are in conflict. Landing times are reassigned by the computer to resolve any time conflicts. The adjusted landing time is referred to as the actual computed landing time. If the ACLT and the ETA are different, the difference indicates the delay that an airplane must accommodate prior to reaching the metering fix through holding, speed control, or path stretching. The ACLT is always greater than or equal to the ETA. The metering fix arrival time assigned to each airplane is computed by subtracting a nominal transition time (from the metering fix to the runway) from the ACLT.

LOCAL FLOW MANAGEMENT/PROFILE DESCENT ALGORITHM DESCRIPTION

The airborne flight management descent algorithm computes the parameters required to describe a five-segment cruise and descent profile (fig. 1) between an arbitrarily located entry fix to an ATC defined metering fix. A sixth segment from the metering fix to the next fix (specified by ATC and called the aim point) is also generated. These parameters are then used by the navigation and display systems to present guidance to the pilot and/or autopilot. The descent profile is based on linear approximations of airplane performance for an idle-thrust, clean-configured descent. Airplane gross weight, wind, and nonstandard temperature and pressure effects are also considered in these calculations.

Figure 1 shows the vertical plane geometry of the path between the entry fix and the aim point. Each path segment from the entry fix to the metering fix is numbered according to the order in which it is calculated by the algorithm. To be compatible with standard airline operating practices, the path is calculated based upon the descent being flown at a constant Mach number with transition to a constant calibrated airspeed and speed changes being flown at constant altitude. The path is flown starting at the entry fix proceeding to the metering fix and aim point.

Segment 5 begins at the entry fix and is flown at a constant cruise altitude and a constant cruise Mach number. Segment 4 is a relatively short path segment in which the speed of the airplane may be changed from the cruise Mach number M_c to the descent Mach number M_d. Segment 4 is eliminated if the descent and the cruise Mach numbers are the same. The descent to the metering fix altitude is accomplished along the next two path segments (segments 3 and 2). Segment 3 is flown at a constant Mach number. As altitude is decreased along this path segment, the calibrated airspeed increases. The desired descent calibrated airspeed is obtained at the beginning of segment 2. The descent is continued along this path segment at a constant calibrated airspeed. When the metering fix altitude has been obtained, the airplane is flown at a constant altitude along segment 1 and slowed from the descent airspeed to the designated metering fix calibrated airspeed. This path segment is eliminated if the descent and metering fix airspeeds are the same. After passing the metering fix, the airplane will be flown directly to the aim point.

The flight management descent algorithm may be used in either of two modes. In the first mode, the pilot may input the Mach/airspeed descent schedule to be flown, and the descent profile is calculated independent of an assigned metering fix time. If a metering fix time is subsequently assigned, some time error, which must be nulled by the pilot, may result since an arbitrary specification of the descent speed schedule may not satisfy both the initial and final time boundary conditions.

The second mode was designed for time-metered operations. In this mode, pilot inputs include the estimated time of arrival to the entry fix and the ATC specified metering fix arrival time. The descent profile is then calculated based on a Mach/CAS descent schedule, computed through an iterative process, that will closely satisfy the crossing times for both of these way points.

Local Flow Management/Profile Descent Algorithm Logic Flow

Figure 2 shows the LFM/PD algorithm logic flow associated with both the time-metered and non-metered modes. Computation of either is initiated by the pilot after he has made his required inputs. In the non-metered mode, where the Mach/CAS descent schedule has been specified by the pilot, way point assigned altitudes and speeds and the path segment times Δt_j and distances Δl_j are computed once and the resulting path is displayed to the pilot.

In the time-metered mode, an appropriate idle-thrust Mach/CAS descent schedule is computed by the algorithm that will satisfy the required entry fix to metering fix transition time Δt_{req}, where

$$\Delta t_{req} = t_{MF} - t_{EF}$$

A check with the following transition time inequality is made to determine that Δt_{req} lies between the minimum and maximum transition time, Δt_{min} and Δt_{max}, to ensure that the descent speed schedule lies within the operational flight envelope of the airplane:

$$\Delta t_{min} \leq \Delta t_{req} \leq \Delta t_{max}$$

Minimum and maximum transition times were calculated by computing the descent profile using maximum and minimum Mach/CAS (0.78/350 knots and 0.62/250 knots, respectively) operational descent speeds as follows:

$$\Delta t_{min} = \sum_{j=1}^{5} \Delta t_j (M_{d,max}, CAS_{d,max})$$

$$\Delta t_{max} = \sum_{j=1}^{5} \Delta t_j (M_{d,min}, CAS_{d,min})$$

If Δt_{req} does not satisfy the transition time inequality, a profile is generated and displayed to the pilot with the limit operational descent speed schedule corresponding to the particular time constraint that was exceeded. The resulting time error is displayed with an appropriate "early or late by" message.

If the transition time inequality is satisfied, an initial Mach/CAS descent schedule is selected. The initial descent airspeed $CAS_{d,i}$ selected is proportional to Δt_{req} and to the total time control available when the descent is flown at the minimum and maximum operational descent speed limits as follows:

$$CAS_{d,i} = \frac{\Delta t_{req} - \Delta t_{min}}{\Delta t_{max} - \Delta t_{min}} (CAS_{d,min} - CAS_{d,max}) + CAS_{d,max}$$

The same time required/time available proportion is used in selecting the initial descent Mach number. However, experience showed that convergence to the final descent speed schedule is quicker when a Mach number slightly larger than one obtained directly with the time proportion is used. The initial descent Mach number is obtained as follows:

$$M_{d,i} = M' + (M_{d,max} - M')/3$$

where

$$M' = \frac{\Delta t_{req} - \Delta t_{min}}{\Delta t_{max} - \Delta t_{min}}(M_{d,min} - M_{d,max}) + M_{d,max}$$

Once the values for the initial Mach/CAS descent speed schedule are selected, an iterative process to arrive at the final descent speed schedule is begun. After completing the first iteration of the profile descent algorithm computations, a convergence test is made to determine whether a satisfactory Mach/CAS descent speed schedule was used. The test consists of checking that the predicted time to fly the profile descent using the selected Mach/CAS descent speed schedule is within 5 seconds of the required time Δt_{req} to fly the descent as follows:

$$\left| \sum_{j=1}^{5} \Delta t_j - \Delta t_{req} \right| \leq 5 \quad \text{sec}$$

If the convergence test is not satisfied, additional iterations are required with appropriate changes to the Mach/CAS descent speed schedule. The descent CAS was incremented or decremented for each iteration as follows:

$$CAS_{d,i+1} = CAS_{d,i} - 0.167 t_E \quad \text{knots}$$

$$CAS_{d,min} \leq CAS_{d,i+1} \leq CAS_{d,max} \quad \text{knots}$$

where

$$t_E = \Delta t_{req} - \sum_{j=1}^{5} \Delta t_j \quad \text{sec}$$

The descent Mach number was not changed unless the descent CAS had reached its maximum or minimum boundary. Then the descent Mach number was changed in 0.01 increments.

Empirical Representation of the TCV Airplane Aerodynamic and Performance Characteristics

Computer memory limitations precluded the use of detailed aerodynamic and performance tables to represent the TCV airplane for profile descent calculations. Instead, an empirical model of airplane performance was developed for a nominal gross weight of 378 080 N (85 000 lb) and standard atmospheric conditions. Gradient techniques were used to modify predicted performance for deviations from the nominal conditions of the empirical model.

The form of the equations that were needed to develop the empirical model were determined from simulator data of a Boeing 737 airplane executing idle-thrust, clean-configured, constant Mach/CAS descents. Actual flight test data were then used to determine the specific numerical constants/parameters that were used in the empirical model of the TCV airplane.

Figure 3 shows altitude rate $\dot{h}$ as a function of altitude h derived from a simulation program of a Boeing 737-100 airplane making 0.73/320 knot and 0.68/250 knot idle-thrust, clean-configured descents. These traces illustrate that, during the constant Mach portion of the descent, altitude rate decreases almost linearly with decreasing altitude. However, the slope $\left(\frac{d\dot{h}}{dh}\right)_{M_d}$ depends upon the magnitude of the descent Mach number. Hence, altitude rate was represented by an equation of the following form:

$$(\dot{h})_{M_d} = \left(\frac{d\dot{h}}{dh}\right)_{M_d} \times h + b \quad \text{m/sec}$$

where b is the magnitude of $\dot{h}$ at sea level. It was observed that each of the linearized constant Mach lines passed through a common point at an altitude 1524 m (5000 ft) above the cruise altitude and at $\dot{h}$ = -9.1 m/sec (-30 ft/sec). The fact that the altitude traces for different descent Mach numbers appeared to intersect about 1524 m above the initial cruise altitude was used to generalize the altitude rate as a function of descent Mach number to arbitrary cruise altitudes below the troposphere (approximately 11 000 m). With this $\dot{h}$ relationship, b may be derived and the equation for altitude rate for constant Mach number descent becomes

$$(\dot{h})_{M_d} = \left(\frac{d\dot{h}}{dh}\right)_{M_d} \times h - \left(\frac{d\dot{h}}{dh}\right)_{M_d} \times (h_c + 1524) - 9.1 \quad \text{m/sec}$$

Figure 4 shows flight data of the variation of $\left(\frac{d\dot{h}}{dh}\right)_{M_d}$ for the TCV airplane during an idle-thrust descent. A quadratic regression analysis was used to obtain the coefficients for the following equation for the variation of $\left(\frac{d\dot{h}}{dh}\right)_{M_d}$ as a function of Mach number:

$$\left(\frac{d\dot{h}}{dh}\right)_{M_d} = A_0 + A_1 \times M_d + A_2 \times M_d^2 \quad (m/sec)/m$$

where

$A_0 = 0.076615$

$A_1 = -0.24125$

$A_2 = 0.193667$

A similar derivation was used to obtain a function for altitude rate for the constant calibrated airspeed portion of the descent. It was found that $\dot{h}$ was approximately constant at all altitudes for a given calibrated airspeed but decreased for an increased airspeed.

Figure 5 shows the idle-thrust descent flight performance data of the TCV airplane for the variation of altitude rate as a function of calibrated airspeed. The following expression was derived through a linear regression analysis to represent the variation of the rate of descent as a function of calibrated airspeed:

$$(\dot{h})_{CAS_d} = -0.09975CAS_d + 14.798 \quad m/sec$$

Figure 6 shows simulator data of a Boeing 737 airplane rate of descent as a function of altitude for a Mach/CAS idle-thrust descent of 0.73/320 knots for three different gross weights. The effects of gross weight variations on the airplane descent performance were accounted for by deriving a multiplication factor to be applied to altitude rate $(\dot{h})_{CAS_d}$ during constant CAS flight and applied to the altitude rate variation with altitude $\left(\frac{d\dot{h}}{dh}\right)_{M_d}$ during the constant Mach region. A linear variation of descent performance as a function of gross weight normalized about a gross weight of 378 080 N resulted in the following equations:

$$K_{\dot{h}} = -0.318697 \frac{GW}{378\ 080} + 1.318697 \qquad \text{(Constant CAS)}$$

$$K_{d\dot{h}/dh} = -0.9207 \frac{GW}{378\ 080} + 1.9207 \qquad \text{(Constant Mach)}$$

Acceleration performance data were required for speed changes at cruise altitudes (FL300 to FL350) and at the metering fix altitudes (5200 m to 6700 m). Figure 7 illustrates the level-flight, clean-configured, idle-thrust deceleration capability as a function of true airspeed of the TCV airplane based on flight test data at typical metering fix altitudes. The following expression was derived through a linear regression analysis so that an average acceleration, in terms of knots/sec, could be calculated given the average true airspeed along a path segment:

$$\ddot{x} = -3.523 \times 10^{-3}\ TAS - 0.10119 \quad \text{knots/sec} \quad (210 \leq TAS \leq 450 \text{ knots})$$

Flight test data also showed that the level-flight, clean-configured, idle-thrust speed changes at cruise altitudes of approximately FL330 to FL350 resulted in a computed constant acceleration of approximately $\ddot{x}_c = -1.15$ knots/sec.

True Airspeed Approximation

It is necessary to determine true airspeed from either Mach number or calibrated airspeed so that a head-wind component can be added to obtain ground speed for time calculations. For Mach number conversion, true airspeed was approximated as a function of altitude h as

$$TAS = M(661 - 7.9723 \times 10^{-3}\ h) \quad \text{knots} \qquad (h \leq 11\ 000 \text{ m})$$

or as a function of static air temperature T_{st} as

$$TAS = 21.64M\sqrt{T_{st}} \quad \text{knots}$$

For calibrated airspeed conversion, true airspeed, considering compressibility and density effects, was approximated as

$$TAS = \frac{CAS}{1 - 0.3937 \times 10^{-4}\, h} \quad \text{knots} \qquad \begin{pmatrix} h \leq 11\,000 \text{ m} \\ 210 \leq CAS \leq 350 \text{ knots} \end{pmatrix}$$

Wind Modeling Technique

A two-segment (upper and lower altitude) linear wind model was used to describe the wind speed and direction between the cruise altitude and the ground. Two gradients for each segment, one showing the variation of wind speed and the other showing the variation of wind direction with changes in altitude, were stored in the computer. A complete wind model for the upper altitude segment (metering fix floor altitude, approximately 5200 m to cruise altitude) was derived by applying the upper altitude gradients to the inertially measured winds at cruise altitude. The lower wind model (surface to the metering fix floor altitude) was derived by applying the lower altitude gradients to the surface winds measured at the airport.

The magnitude of each gradient was derived from the winds-aloft forecast for the test area and stored in the computer before each flight. The surface wind at the airport was inserted by the pilot through the NCDU prior to each descent. The magnitude of the wind velocity at cruise altitude was the value measured by the inertial system at the time of the initial profile descent calculation.

The following linear equations were used to determine the magnitude of the wind velocity at any altitude h:

$$(S_w)_h = \left(\frac{dS_w}{dh}\right)_H (h - h_c) + S_{w,c} \quad \text{knots} \qquad (h \geq \text{Metering fix floor altitude})$$

$$(D_w)_h = \left(\frac{dD_w}{dh}\right)_H (h - h_c) + D_{w,c} \quad \text{deg} \qquad (h \geq \text{Metering fix floor altitude})$$

$$(S_w)_h = \left(\frac{dS_w}{dh}\right)_L (h - h_{grd}) + S_{w,grd} \quad \text{knots} \qquad (h < \text{Metering fix floor altitude})$$

$$(D_w)_h = \left(\frac{dD_w}{dh}\right)_L (h - h_{grd}) + D_{w,grd} \quad \text{deg} \qquad (h < \text{Metering fix floor altitude})$$

The head-wind component at an altitude h was then computed for a specific ground track angle TRK by using the relation:

$$(W_H)_h = (S_w)_h \cos (D_w)_h - TRK \quad \text{knots}$$

Compensation for Nonstandard Atmospheric Temperature and Pressure Effects

Various flight instruments including the Mach meter, airspeed indicator, and the altimeter are designed to display correct indications in a standard atmosphere. However, standard atmospheric conditions are rarely encountered which result in slight errors in indicated altitude and speed. The LFM/PD algorithm compensates for nonstandard temperatures as they affect altimeter indications and the speed-of-sound calculations. Compensation is also applied to altimeter indications for nonstandard pressure effects.

The international standard atmosphere temperature model is shown in figure 8 as a solid line. This linear model has a standard sea-level temperature T_o of 288 K and a temperature lapse rate a of -0.00649 K/m. The LFM/PD algorithm defines a new temperature model shown in figure 8 as a dashed line utilizing the standard temperature lapse rate but incorporating a nonstandard sea-level temperature T_o'. The nonstandard sea-level temperature is determined by summing the temperature measured at cruise altitude with the product of the temperature lapse rate and cruise altitude.

The nonstandard sea-level temperature is used to define a relationship between the indicated altitude displayed to the pilot and the geopotential altitude used in the descent path calculations. The pressure altitude indicated by a barometric altimeter is given by

$$h_p = \frac{T_o}{a}\left[\left(\frac{p_{st}}{p_o}\right)^{-aR} - 1\right] + \Delta h_p \quad \text{m}$$

If the temperature lapse rate is assumed constant, the estimated pressure altitude with nonstandard sea-level temperature may be approximated by

$$h_p' = \frac{T_o'}{a}\left[\left(\frac{p_{st}}{p_o}\right)^{-aR} - 1\right] + \Delta h_p \quad \text{m}$$

The approximate altitude error due to nonstandard temperature effects Δh_T is determined by subtracting h_p' from h_p with the error due to nonstandard pressure effects Δh_p assumed to be zero, and the following equation results:

$$\Delta h_T = h_p\left(1 - \frac{T_O'}{T_O}\right) \quad m$$

Compensation for nonstandard sea-level pressure effects on indicated altitude was approximated by using the relation that 33.86 mb (1 in. of mercury) is equivalent to 304.8 m (1000 ft) of altitude. Therefore, the altitude error is given by

$$\Delta h_p = -9.002(BARO - 1013.2) \quad m$$

where BARO is the barometric altimeter setting in millibars.

Combining the nonstandard temperature and pressure corrections results in the following expressions to determine the approximate geopotential altitude h_{GP} from an indicated altitude h_I or conversely to determine the approximate indicated altitude corresponding to a given geopotential altitude. The distinction between altitudes above and below FL180 results from the operational use of "pressure altitude" obtained by setting the altimeter to 1013.2 mb when flying above FL180. The pressure correction is not required below FL180 since the altimeter would be reset to a nearby station value; thus, the indicated altitude would already contain the pressure correction. These equations are

$$h_{GP} = h_I\left(2 - \frac{T_O'}{288.2}\right) \quad m \qquad (h \leqq FL180)$$

$$h_{GP} = [h_I + 9.002(BARO - 1013.2)]\left(2 - \frac{T_O'}{288.2}\right) \quad m \qquad (h > FL180)$$

$$h_I = \frac{h_{GP}}{\left(2 - \frac{T_O'}{288.2}\right)} \quad m \qquad (h \leqq FL180)$$

$$h_I = \frac{h_{GP}}{\left(2 - \frac{T_O'}{288.2}\right)} - 9.002(BARO - 1013.2) \quad m \qquad (h > FL180)$$

Descent Path Computations

The cruise and descent path between the entry fix and the aim point was defined by computing the relative location and altitude of the necessary intermediate way points. The altitude of each way point was computed first. Ground speed at which the airplane was to cross each way point was determined by summing the result of the Mach number or CAS to true airspeed conversions with the head-wind component derived from the wind model. Then the relative locations of the way points were determined by computing the length of the path segments between the way points. On the level-flight path segments, the assigned way point ground speeds and the airplane deceleration capability were used. On the descent path segments, the average rate of descent $\dot{h}$ and the required altitude change were used to determine the time to travel between the way points. This path segment time was combined with the average segment ground speed to determine the segment length. The details of these calculations are presented in the following paragraphs.

Metering fix altitude.- The first requirement was to determine the desired metering fix altitude that would enable the TCV Boeing 737 airplane to descend from the metering fix to the aim point in an idle-thrust, clean configuration. The geopotential metering fix altitude is given by

$$h_{MF} = h_{AP} + 3600 l_{AP} \frac{\dot{h}}{TAS - (W_H)_h} \quad m$$

The altitude rate $\dot{h}$ was determined by using the empirical expression shown in figure 5 compensated for gross-weight effects. The true airspeed TAS is the average of the metering fix and aim point calibrated airspeeds converted to true airspeed at the average assigned altitude between the metering fix and aim point. The head wind $(W_H)_h$ was also determined at this average altitude.

The geopotential metering fix altitude was then converted to an indicated altitude and limited to fall within the published metering fix altitude window.

The desired metering fix altitude must be limited to comply with published profile descent procedures to assure that adequate airspace for departure and overflight traffic is maintained. The need to limit the desired metering fix altitude usually results from operating in the presence of an extreme head wind/tail wind. The impact on the profile descent flight technique is that one or more of the assumed preconditions (idle thrust, flaps zero, and gear and speed brakes retracted) must be violated to fly between the metering fix and the aim point.

Mach/CAS transition altitude.- A way point was positioned in the descent to denote the point that the pilot would transition from a constant Mach number descent to a constant calibrated airspeed descent. The general equation for altitude of the transition way point was determined by setting the expressions for true airspeed as a function of calibrated airspeed and as a function of

Mach number equal to each other and solving for geopotential altitude. The resultant transition altitude is given by

$$h_{XO} = 54155 - \left\{2.933 \times 10^9 - \left[3.1861 \times 10^6\left(661 - \frac{CAS_d}{M_d}\right)\right]\right\}^{1/2} \quad m$$

$$(h_{MF} \leq h_{XO} \leq h_c)$$

Segment 1.- Path segment 1 is a level-flight segment on which the airplane is slowed from the descent calibrated airspeed to arrive at the metering fix at a CAS of 250 knots. If the descent airspeed is equal to a CAS of 250 knots, the segment 1 time and length are set equal to zero and the segment 2 computations are started.

The equations for segment 1 time and length are

$$\Delta t_1 = \frac{(CAS_d - 250)}{\ddot{x}(1 - 0.3937 \times 10^{-4}\, h_{MF})} \quad sec$$

$$\Delta l_1 = \left[\frac{(CAS_d + 250)/2}{1 - 0.3937 \times 10^{-4}\, h_{MF}} - (W_H)_{h_{MF}}\right]\frac{\Delta t_1}{3600} \quad n.\ mi.$$

The acceleration $\ddot{x}$ along segment 1 is evaluated with an average of the true airspeeds obtained at the segment beginning and ending way points.

Segment 2.- Segment 2 is a constant calibrated airspeed descent flown at idle-thrust power settings. The equations for the time and length of segment 2 are

$$\Delta t_2 = \frac{(h_{XO} - h_{MF})}{\dot{K_h}(-0.09975CAS_d + 14.798)} \quad sec$$

$$\Delta l_2 = \left[\frac{CAS_d}{1 - 0.3937 \times 10^{-4}\,\frac{(h_{XO} + h_{MF})}{2}} - (W_H)_{\frac{h_{XO}+h_{MF}}{2}}\right]\frac{\Delta t_2}{3600} \quad n.\ mi.$$

The time relationship Δt_2 is given by an altitude change (difference in the geopotential altitudes of the way points defining the segment) divided by an altitude rate corrected for gross-weight effects with the $K_{\dot{h}}$ multiplication factor. The conversion from calibrated to true airspeed and the head-wind component are computed based on the average of the transition and the metering fix altitudes.

Segment 3.- Segment 3 is a constant Mach descent flown at idle-thrust power settings. The constant Mach segment is described by a first-order differential equation of the form

$$(\dot{h})_h + K_1 h + K_2 = 0$$

This equation results directly from the altitude rate relationship for constant Mach number descents previously discussed. The resulting time and distance relations are

$$\Delta t_3 = \frac{\ln[(K_2 + K_1 h_c)/(K_1 h_{XO} + K_2)]}{K_1} \quad \text{sec}$$

$$\Delta l_3 = \left[21.64 \sqrt{T_{st,3}} M_d - (W_H)_{\frac{h_c + h_{XO}}{2}} \right] \frac{\Delta t_3}{3600} \quad \text{n. mi.}$$

where $-K_1$ is the change in altitude rate with altitude, evaluated at the descent Mach number, corrected for gross-weight effects with the multiplication factor $K_{d\dot{h}/dh}$ as follows:

$$K_1 = -(K_{d\dot{h}/dh}) \left[\left(\frac{d\dot{h}}{dh} \right)_{M_d} \right] \quad (\text{m/sec})/\text{m}$$

and K_2 is given by the following empirical relation:

$$K_2 = 9.1 - K_1 (h_c + 1524) \quad \text{m/sec}$$

The static temperature $T_{st,3}$ and the head-wind component are evaluated at the average geopotential altitude between cruise and transition way-point altitudes.

Segment 4.- Segment 4 is a level-flight speed change from the cruise Mach number to the descent Mach number. If the descent Mach number is within ±0.015 of the cruise Mach number, the segment time and length are set to zero; otherwise,

$$\Delta t_4 = 21.64\sqrt{T_{st,4}}\,\frac{|M_c - M_d|}{\ddot{x}_c} \quad \text{sec}$$

$$\Delta l_4 = \left[21.64\sqrt{T_{st,4}}\,\frac{(M_c + M_d)}{2} - (W_H)_{h_c}\right]\frac{\Delta t_4}{3600} \quad \text{n. mi.}$$

The time relation Δt_4 is a true airspeed change divided by an acceleration $\ddot{x}_c$ which was determined to be a constant -1.15 knots/sec. Static temperature $T_{st,4}$ is determined at cruise altitude and the head-wind component is computed for cruise altitude.

Segment 5.- Segment 5 is the remaining path between the entry fix and the beginning of segment 4. The length of segment 5 Δl_5 is simply the difference between the total distance between the entry fix and metering fix l_t and the sum of the distances of the remaining four segments and is given as follows:

$$\Delta l_5 = l_t - \sum_{j=1}^{4} \Delta l_j \quad \text{n. mi.}$$

Segment time Δt_5 is found by dividing the distance to be flown by the ground speed as follows:

$$\Delta t_5 = \frac{3600\,\Delta l_5}{21.64\sqrt{T_{st,5}}M_c - (W_H)_{h_c}} \quad \text{sec}$$

The static temperature is determined at cruise altitude and the head wind computed for the geopotential cruise altitude.

Input/Output Requirements

Data required for profile descent calculations are obtained from the NCU navigation data base, from pilot inputs through the NCDU, and from real-time sensor inputs through a data bus to the NCU.

Parameters contained in the NCU navigation data base include

(1) Aim point: location (latitude and longitude), programmed altitude, and programmed airspeed

(2) Metering fix: location (latitude and longitude), maximum and minimum programmed altitudes, and programmed airspeed

(3) Maximum and minimum airplane operational descent Mach number and airspeed

(4) Wind speed and direction gradients

Inputs required for the profile descent calculations inserted through the NCDU by the pilot include

(1) Entry fix description: location, programmed altitude, programmed ground speed, and programmed crossing time; the entry fix is the last way point the pilot has defined on his path before using the LFM/PD algorithm

(2) Descent Mach/CAS schedule (not required if both the metering fix and entry fix times are specified)

(3) Metering fix time (not required if the pilot selects the descent Mach/CAS schedule)

(4) Surface winds

(5) Airport altimeter setting

(6) Airplane gross weight

(7) Total air temperature

Information required for the profile descent calculations input to the navigation computer automatically through a data bus include (magnitudes at time of profile descent calculation)

(1) Winds-aloft speed and direction

(2) Cruise Mach number

(3) Cruise altitude

The flight management descent algorithm calculates and outputs the following parameters to be used by the guidance and display system:

(1) All descent way-point distances relative to the metering fix, programmed altitudes, and programmed ground speeds

(2) The magnetic direction of the entry fix relative to the metering fix (all way points used to describe the descent profile lie in the vertical plane defined between the metering fix and entry fix)

(3) Mach/CAS descent schedule

FLIGHT TEST OBJECTIVES

The objectives of the flight tests were to (1) document the descent path parameters determined by the descent flight management algorithm including wind modeling effects, (2) determine the compatibility of the airborne flight management descent concept with time control in the cockpit while operating in the time-based metered LFM/PD air traffic control environment, (3) determine pilot acceptance of the cockpit procedures to program and fly a fuel-conservative, time-controlled descent, and (4) obtain data for estimates of fuel usage. These objectives were achieved by using qualitative data in the form of pilot and ARTCC radar controller comments; audio recordings of controller, cockpit, and air-to-ground conversations; and video recordings from the ARTCC radar scope and by using quantitative data in the form of speed, altitude, and time error recorded onboard the airplane.

DESCRIPTION OF AIRPLANE AND EXPERIMENTAL SYSTEMS

The test airplane is the TCV Boeing 737 research airplane (a twin-engine subsonic jet commercial transport). The experimental systems consist of a triplex digital flight control system, a digital navigation and guidance system, and an electronic CRT display system that is integrated into a separate research flight deck (ref. 6). The full-scale research flight deck is located in the airplane cabin just forward of the wing as shown in figure 9. Figure 10 shows the instrument panel of the research flight deck.

The triply redundant digital flight control system provides both automatic and fly-by-wire control wheel steering options. The velocity vector control wheel steering mode (ref. 6) was utilized during these flight tests. In this control mode, the flight control computers vary pitch attitude and heading to maintain flight-path angle and track angle, respectively.

The navigation computer is a general-purpose digital computer designed for airborne computations and data processing tasks. It utilizes a 24-bit word length and has a 32 000-word directly addressable core memory. Major software routines (refs. 7 and 8) in the navigation computer include (1) navigation position estimate, (2) flight route definition, (3) guidance commands to the flight control computer system, (4) piloting display system computations, and

(5) flight data storage for navigation purposes. The flight management descent algorithm software was also included in the navigation computer.

The captain and the first officer each have three CRT displays and conventional airspeed and altimeter instrumentation for guidance. The three CRT displays include the EADI, the EHSI, and the NCDU which is a digital display of various navigation information stored in the NCU.

The EADI display is formatted much like a conventional attitude indicator but has additional symbology to help the pilot navigate and control the airplane. A detailed explanation of the EADI display may be found in reference 7. Two options of the EADI display used for lateral and vertical path navigation on these flight tests are the vertical and lateral course deviation indicators and the star indicator used with the flight-path angle wedges as shown in figure 11.

The vertical and lateral course deviation indicators are presented in a conventional needle and tape format. The vertical tape on the right-hand side of the EADI shows the vertical path error. A standard "fly to" deviation convention is employed where the needle represents the desired path and the center of the tape represents the airplane (i.e., if the airplane is below the desired path the needle will be displaced above the center of the tape). The indicated range of the tape scale is ±152 m (±500 ft). The lateral course deviation indicator is displayed on the bottom of the EADI. The fly to deviation convention is also utilized and the indicated range of the horizontal tape is ±1829 m (±6000 ft).

The second EADI navigation option used during this test was the star indicator used with the flight-path angle wedges shown in figure 11. The star represents the next way point on the programmed route. The star's vertical displacement on the EADI pitch grid represents the flight-path angle at which the airplane must be flown to arrive at the programmed altitude at the next way point. The star is also displaced laterally to provide lateral path tracking guidance.

The flight-path angle wedges used with the star display represent the inertially referenced flight path of the airplane. If the airplane flight-path angle and track angle are adjusted so that the flight-path angle wedges center directly on the star, the airplane will be flying directly to the way point.

Figure 12 is a drawing of the EHSI display operated in a track-up mode. This display is a plan view of the desired route and optionally displayed features such as radio fixes, navigation aids, airports, and terrain drawn relative to the airplane's position indicated by a triangular airplane symbol. A trend vector is displayed in front of the airplane symbol to aid the pilot with route capture and tracking and with time guidance utilization. The trend vector is composed of three consecutive lines which predict where the airplane will be in the next 30, 60, and 90 sec based on the airplane's current ground speed and bank angle. The EHSI display also provides the pilot with time guidance and an altitude predictive arc to aid the pilot during altitude changes.

Time guidance is provided on the EHSI by a box symbol that moves along the programmed path. The time box represents the position along the route where the airplane should be based on the programmed ground speeds and the time profile. The pilot nulls the time error by maneuvering the airplane so that the airplane symbol is contained within the time box.

During climbs and descents, the pilot may select the range/altitude arc symbol to be drawn on the EHSI as shown in figure 12. This symbol depicts the range in front of the airplane where a pilot-selected reference altitude will be achieved based on the airplane's current altitude and flight-path angle and the desired reference altitude.

The range/altitude arc was used on the descent profile during these tests by setting the magnitude of the reference altitude to the programmed altitude of the next way point. Then the pilot would adjust the flight-path angle of the airplane so that the arc would lie on top of the next way point displayed on the EHSI. This resulted in the airplane crossing the next way point at the programmed altitude.

The NCDU display contains numerous navigational data for the pilot to select including programmed route information, tracking and navigational error information, and systems status checks. This information is presented in alphanumeric form. A complete description of the NCDU and its operations may be found in reference 7.

DATA ACQUISITION

Data were recorded onboard the airplane by a wide-band magnetic tape recorder at 40 samples/sec. These data included 93 parameters describing the airplane configuration, attitude, control surface activity, and 32 selectable parameters from the navigation computer. Airborne video recordings of the EADI and the EHSI displays were made throughout each flight. In addition, audio records of test crew conversations and air/ground communications were recorded.

On the ground, the ATC radar controller's scope presentation and the Air Route Traffic Control Center computer-generated time-based metering update list were video recorded.

FLIGHT TEST CREW

The flight test crew consisted of a captain and first officer. The captain was responsible for flying the airplane in the velocity vector control wheel steering mode and for operation of the thrust levers. The first officer was responsible for program inputs to the navigation computer, selecting appropriate display guidance, and assisting the captain as requested. In addition, the first officer recorded flight notes of various parameters describing the profile descent for postflight analysis.

Two NASA test pilots and four management/line airline pilots served as captain during the flight tests. Both NASA pilots had extensive previous flight and simulation experience with the TCV airplane and its experimental flight control and display systems. The four airline pilots each had approximately 6 hours of simulator training prior to the flight tests. One of the airline pilots had 4 hours of flight time in the TCV airplane acquired during unrelated flight tests 9 months earlier.

A NASA engineer served as first officer on all flights. He had previous flight crew experience in simulation and flight with the TCV airplane and its experimental systems.

TASK

Other than requiring the time navigation responsibility to be in the cockpit, the experiment task required the flight crew to operate the airplane as a normal arrival flight to the Denver airport participating in the time-based metered LFM/PD air traffic control system. Each test run was started with the airplane at cruise altitude and speed on a 4-D programmed path to an entry fix 110 n. mi. from Denver. Prior to passing the entry fix, the flight crew received a profile descent clearance and an assigned metering fix time from the Denver ARTCC. The flight crew then keyed the appropriate parameters into the NCDU so that an idle-thrust descent path to the metering fix would be generated and displayed. Then the crew flew to the metering fix using 4-D path guidance presented on the EADI and EHSI displays. Each test run was terminated at the metering fix and the airplane was repositioned for another test run (or flown back to the airport after the final test of the day).

The flight crew was expected to null lateral and vertical path errors throughout the test and null the time error prior to the top-of-descent way point. During the descent to the metering fix, thrust was retained at flight idle, and speed brakes were not used regardless of any time error so that the effects of wind modeling on the predicted descent path could be observed. Path deviations for air traffic control purposes or due to weather were accepted and accommodated during the test runs.

The flight test path, including the profile descent segments, flown for each run is shown in figure 13. This test path was 420 n. mi. long and took approximately 1 hour to fly. The first officer would program path guidance to the entry fix prior to arriving at the Gill VORTAC. After the final metering fix arrival time was computed by the Denver ARTCC and radioed to the airplane, guidance for the profile descent between the entry fix and the aim point was computed with the navigation computer by using the flight management descent algorithm.

The pilot was instructed to null small time errors (less than 20 sec) through speed control and larger time errors through path stretching (with ATC concurrence) maneuvers. However, the pilot was to have attained the programmed ground speed and altitude at the top-of-descent way point regardless of the time error.

Between the top-of-descent and the metering fix way points, the airplane was flown at idle thrust and the use of speed brakes was not permitted. The captain used path guidance on the EHSI display and the lateral path deviation indicator on the EADI for lateral path guidance. For vertical guidance, the star and flight-path angle wedges on the EADI and the range altitude arc on the EHSI display were used. It was the responsibility of the first officer to select the desired altitude for the range/altitude arc option so that the captain could devote full attention to flying the airplane.

Use of the vertical guidance in this fashion resulted in the airplane being flown in the vertical plane along a straight line between way points. Even through a constant Mach descent requires an increased rate of descent as altitude is lost, the straight-line flight path results in little error.

The captain would anticipate leveling the airplane for the programmed altitude at the bottom-of-descent way point with reference to a conventional barometric altimeter and then would proceed to the metering fix. After passing the metering fix, the test run was complete and the captain would turn the airplane to reposition for another test run.

RESULTS AND DISCUSSION

Airborne Algorithm Flight Performance

The prime indicator of performance of the flight management descent algorithm and concept of time control in the cockpit was the accuracy in terms of time, airspeed, and altitude with which the airplane passed the metering fix. This accuracy was quantified through the calculation of the mean and standard deviation of the altitude error, airspeed error, and time error for 19 test runs.

The mean, standard deviation, and maximum value for the altitude, airspeed, and time errors are summarized in the following table:

	Altitude error, m (ft)	CAS error, knots	Absolute time error, sec
Mean	10.2 (33.6) high	0.3 slow	6.6 late
Standard deviation	23.7 (77.8)	6.5	12.0
Maximum error	51.5 (169) high	12.9 fast	29.0 late

The values of these errors were judged by the pilots to be very good for this flight environment. These data demonstrated that highly accurate fuel efficient descent profiles that satisfy terminal time boundary constraints can be generated and flown using a relatively simple and straight-forward empirical

model for the aerodynamic and performance characteristics of the airplane. Because of the simplicity of modeling these characteristics, this algorithm could be applied to various flight management/planning systems that are much less sophisticated than the NASA TCV Boeing 737 experimental system.

The standard deviation and the maximum value of the altitude error was slightly higher than expected. This was attributed to the fact that the pilots had been instructed not to make minor altitude corrections after the initial level-off at the bottom-of-descent way point so that the difference between the actual and predicted airspeed change between the bottom-of-descent and metering fix way points could be accurately assessed.

The absolute time error of the airplane crossing the metering fix resulted in a significant error reduction with time control in the cockpit. The pilots felt that they could have reduced the time error even further had they been allowed to modulate thrust and speed brakes during the descent. Since the thrust was at flight idle and the speed brakes not employed during the descent, the absolute time error was a function of the initial time error at the top of descent as well as a function of the flight management descent algorithms (which included wind modeling).

The time error accumulated between the top-of-descent and the metering fix way points more appropriately reflects the accuracy with which the performance of the airplane and the winds had been modeled in the flight management descent algorithm. The mean and standard deviation of the accumulated time error for the 19 test runs was 2.5 sec and 6.9 sec, respectively. The maximum accumulated time error was 15 sec but typically less than 9 sec.

The mean and standard deviation of the time errors associated with crossing the metering fix may have been influenced by the time error in the Mach/CAS descent speed schedule convergence test. During these flights, the descent speed schedule was computed based upon a 5-sec time error convergence criterion. Five sec was chosen because the descent speed schedule could be computed in less than six iterations and would result in a reasonable bound upon the time error with the resulting descent speed schedule. However, if more computational iterations to compute the descent speed schedule are permissible, then the convergence criterion could be reduced and a corresponding reduction of time error crossing the metering fix expected.

Wind Modeling

The two-segment linear wind model was designed to provide a simple representation of the winds that would minimize the time error of the airplane crossing the metering fix. This was accomplished by using forecasted wind information to define the speed and direction wind model line gradients and by using wind velocities measured at the airport (surface winds for the lower wind segment) and at cruise altitude (inertially measured winds for the upper wind segment) to position these line gradients and complete the wind model. This type of representation minimized the impact of wind modeling errors since most of the time flying between the entry fix and metering fix was at cruise altitude where wind modeling was most accurate. Wind modeling errors that

occurred during the descent were attenuated by the relatively short exposure time to improperly modeled winds.

The direction and speed gradients of the two-segment linear wind model were entered into the descent flight management software each day prior to flight. The gradients for the wind model were based on the winds-aloft forecast for the Denver area for the time period of the test flights. Since the winds-aloft forecast was made 6 to 8 hr before the flight tests, actual winds aloft were measured and recorded onboard during the climb to cruise altitude on the first test run of the day. This wind information was plotted and compared to the forecast to determine if the wind model gradients should be modified. The gradients could be changed in flight for succeeding test runs, if required. The wind speed gradient was changed on only two of the test runs - one of these changes is shown in figure 14.

Figure 14 shows the original and modified wind models used and the winds measured for two consecutive test runs. The first test run used a model based on the winds-aloft forecast obtained before the flight. The second run used a wind model based on the winds measured during the first test run. The wind speed gradient on the first model resulted in predicted wind speeds (modeled) to be faster than actual speeds encountered during the descent. The accumulated time error resulting on this run was 15 sec. The gradient of the wind speed model was increased for the second test run while the direction gradient was unchanged. The resulting accumulated time error was reduced to 2 sec.

Figure 14 also shows the inertially measured wind speed and direction (circled data points) used to complete the wind model definition. These data points were measured at the time of the descent calculation. During these test flights this point of calculation was typically 100 n. mi. before the top-of-descent way point. This resulted in the possibility of a bias error in the modeled wind speed and/or direction due to a wind shift between the point where the descent calculation was executed and the top of descent. This phenomena occurred in the direction gradient of the second run as shown in figure 14. The measured wind direction at the point of descent calculation (115 n. mi. from the top of descent) was 304°, and at the top of descent, the measured wind direction was 291°. Hence, a 13° bias error in direction resulted during the descent.

Airborne and Ground System Compatibility

The profile descent calculated by the flight management descent algorithm, pilot's guidance, and cockpit procedures were designed to be compatible with current time-based metering LFM/PD ATC procedures and with other traffic participating in the ATC system. The test airplane was treated by the automated time-based metering LFM/PD computer program in the same manner as other airplanes inbound to the Denver airport. The only ATC procedural difference during the flight tests was that the test airplane pilots were given the assigned metering fix time since they were responsible for time management, which resulted in no path stretching radar vectors or speed control commands required for sequencing purposes. Controller comments

indicated that this difference allowed a reduction in their workload due to less required ground-to-air radio transmissions.

Pilot comments indicated that the task of flying profile descents with time control with the electronic displays was very easily accomplished. The descent algorithm and the path guidance substantially reduced the pilot's workload, no cockpit calculations were required to determine the top-of-descent way point, and guidance presented to the pilot made it easy to maintain accurate time control. Computer inputs prior to descent were direct and simple.

Video tape recordings of the ATC controller's radar scope have shown that the test airplane operated compatibly with other traffic. The TCV airplane merged with, and remained in, a queue of other airplanes bound for the metering fix. This compatibility resulted because of the Mach/airspeed descent schedule and resulting time profile calculated with the descent management algorithm based on the assigned metering fix time. This assigned metering fix time was based upon the position and metering fix time assigned to the airplanes landing prior to the TCV airplane. Proper spacing between these airplanes and the test airplane would result if the time profile was followed.

Fuel Savings

Fuel savings are accomplished on both a fleet-wide basis and an individual airplane basis. Time-based metering procedures produce fleet-wide fuel savings by reducing extra vectoring and holding of airplanes at low altitude for sequencing into an approach queue. Profile descent procedures produce individual airplane fuel savings by allowing the pilot to plan for a fuel efficient descent to the metering fix.

No attempt was made to quantify the increased fleet-wide fuel savings due to the reduction of time dispersion crossing the metering fix since the TCV airplane was the only airplane that utilized onboard-generated 4-D guidance during these tests. It is apparent, however, that a reduction in time dispersion between airplanes being merged into an approach queue can produce an increase in fuel savings by a reduction in extra maneuvering for longitudinal spacing and can produce an increase in runway utilization by reducing excessively large time separation between airplanes.

Fuel savings at the Denver airport as a result of today's profile descent operations has been estimated to be as high as three and a quarter million dollars per year (ref. 5). Additional fuel savings as a result of the airborne algorithms were quantified through an analytical comparison of a descent calculated by the flight management descent algorithm and a conventional descent typical of those airplanes observed on the ARTCC radar display. Fuel use for each descent was based on fuel flow for a Boeing 737 airplane.

Figure 15 shows the vertical profile of both the calculated and conventional descents. Identical initial and final boundary conditions (location, altitude, speeds, and transition time) were used for both descents so that a valid comparison of fuel use could be made. Both descents begin at the entry

fix, 76 n. mi. from the metering fix, at an altitude of FL350, and at a cruise Mach number of 0.78. The descents end at the metering fix at an altitude of FL195 and at a calibrated airspeed of 250 knots. Flying time for both descents is 11.7 min.

The conventional descent is based on idle thrust at a Mach number of 0.78 with a transition to a CAS of 340 knots. The descent from cruise altitude is started at a point 60 n. mi. from the metering fix which is consistent with various pilot rules of thumb for descent planning. At the bottom of descent, the airplane is slowed until it reaches a calibrated airspeed of 250 knots. Thrust is then added as required to maintain the airspeed at 250 knots.

The descent calculated by the flight management descent algorithm is based upon an 11.7-min time constraint. The calculated Mach/CAS descent schedule for this profile is 0.62/250 knots. Thrust is set to flight idle approximately 7 n. mi. prior to the descent so that the airplane may slow from the cruise to the descent Mach number. A descent segment at a constant Mach number of 0.62 is started 40.6 n. mi. from the metering fix with transition to a descent segment at a constant CAS of 250 knots to the metering fix.

Both descents, by definition of the comparison, require the same amount of time to fly between the entry fix and the metering fix. This time objective is achieved with similar ground speeds on both descents. Even though the calculated descent is flown at a slower indicated Mach/CAS descent schedule, similar ground speeds result since the airplane stays at altitudes higher than on the conventional descent.

Fuel usage on these two descents is substantially different, however. The descent calculated by the flight management descent algorithm required approximately 28 percent less fuel to fly between the entry fix and the metering fix (2989 N (672 lb) on the conventional descent and 2148 N (483 lb) on the calculated descent). Approximately two-thirds of this fuel savings was attributed to the lower indicated airspeeds and one-third to flight at higher altitudes.

CONCLUDING REMARKS

A simple airborne flight management descent algorithm designed to define a flight profile subject to the constraints of using idle-thrust, a clean airplane configuration (landing gear up, flaps zero, and speed brakes retracted), and fixed time end conditions was developed and flight-tested in the NASA TCV Boeing 737 research airplane. The research test flights, conducted in the Denver ARTCC automated time-based metering LFM/PD ATC environment, demonstrated that time guidance and control in the cockpit was acceptable to the pilots and ATC controllers and resulted in arrival of the airplane over the metering fix with standard deviations in airspeed error of 6.5 knots, in altitude error of 23.7 m (77.8 ft), and in arrival time accuracy of 12 sec. These accuracies indicated a good representation of airplane performance and wind modeling. Fuel savings will be obtained on a fleet-wide basis through a reduction of the time error dispersions at the metering fix and on a single airplane basis by presenting the pilot guidance for a fuel efficient descent. Pilot workload

was reduced by eliminating the need for rules of thumb and/or extensive experience to achieve a solution to a complex four-dimensional (4-D) navigation problem and through steering guidance for 4-D path following. ATC controller workload was reduced through a reduction of required ground-to-air communications and through the transfer of time navigation responsibilities to the cockpit.

Langley Research Center
National Aeronautics and Space Administration
Hampton, VA 23665
August 19, 1980

REFERENCES

1. Stein, Kenneth J.: New Procedures Key to Fuel Savings. Aviat. Week & Space Technol., vol. 111, no. 9, Aug. 27, 1979, pp. 105-111.

2. Stein, Kenneth J.: Advanced Systems Aid Profile Descents. Aviat. Week & Space Technol., vol. 111, no. 8, Aug. 20, 1979, pp. 57-62.

3. Ames Research Center and Aviation Safety Reporting System Office: NASA Aviation Safety Reporting System: Fifth Quarterly Report April 1 - June 30, 1977. NASA TM-78476, 1978.

4. Heimbold, R. L.; Lee, H. P.; and Leffler, M. F.: Development of Advanced Avionics Systems Applicable to Terminal-Configured Vehicles. NASA CR-3280, 1980.

5. Cunningham, F. L.: The Profile Descent. AIAA Paper 77-1251, Aug. 1977.

6. Staff of NASA Langley Research Center and Boeing Commercial Airplane Company: Terminal Configured Vehicle Program - Test Facilities Guide. NASA SP-435, 1980.

7. Cosley, D.; and Martin, A. J.: ADEDS Functional/Software Requirements. SST Technology Follow-On Program - Phase II. Rep. No. FAA-SS-73-19, Dec. 1973. (Available from DTIC as AD B000 287.)

8. McKinstry, R. Gill: Guidance Algorithms and Non-Critical Control Laws for ADEDS and the AGCS. Doc. D6-41565, Boeing Co., 1974.

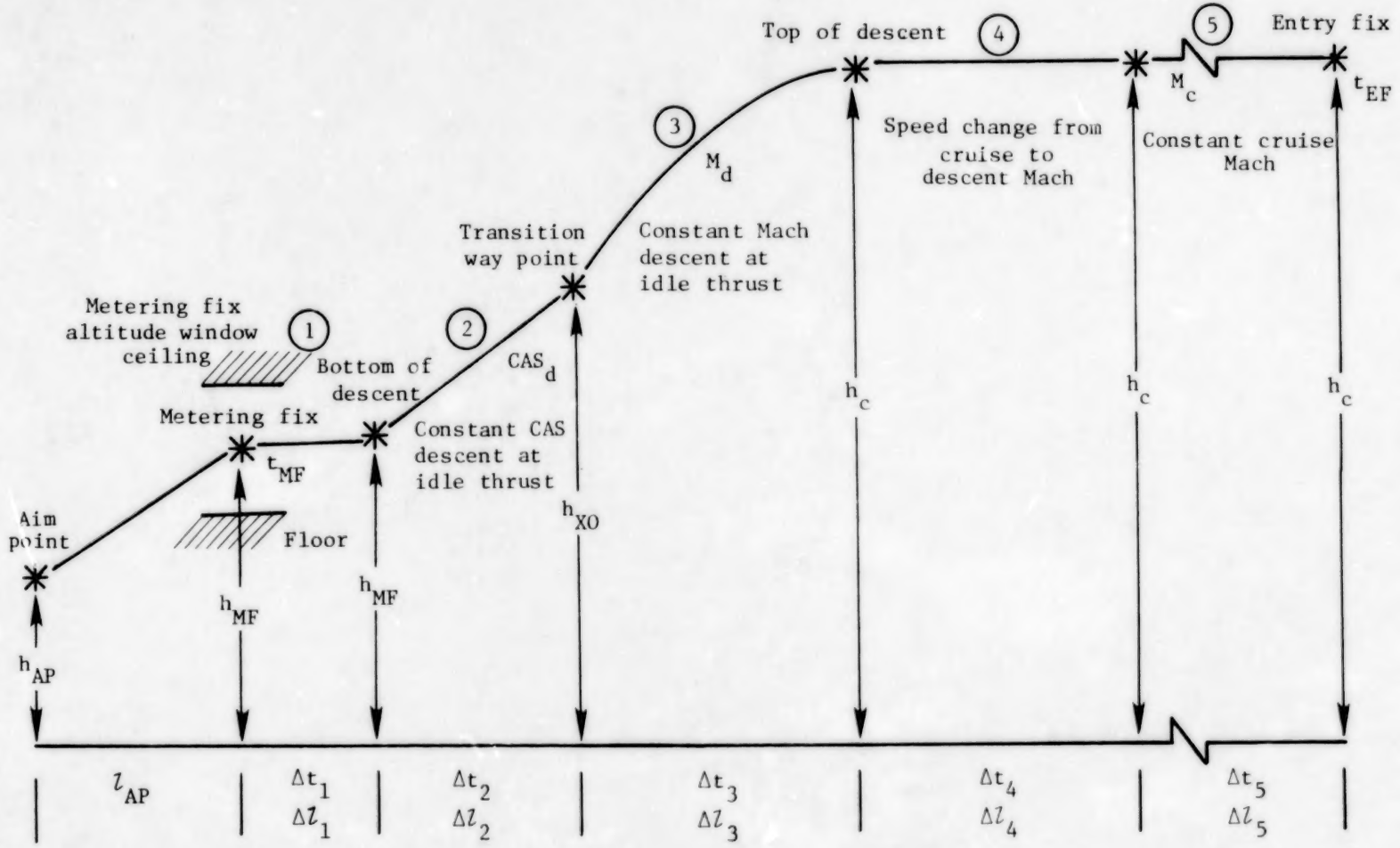

Figure 1.- LFM/PD vertical plane geometry.

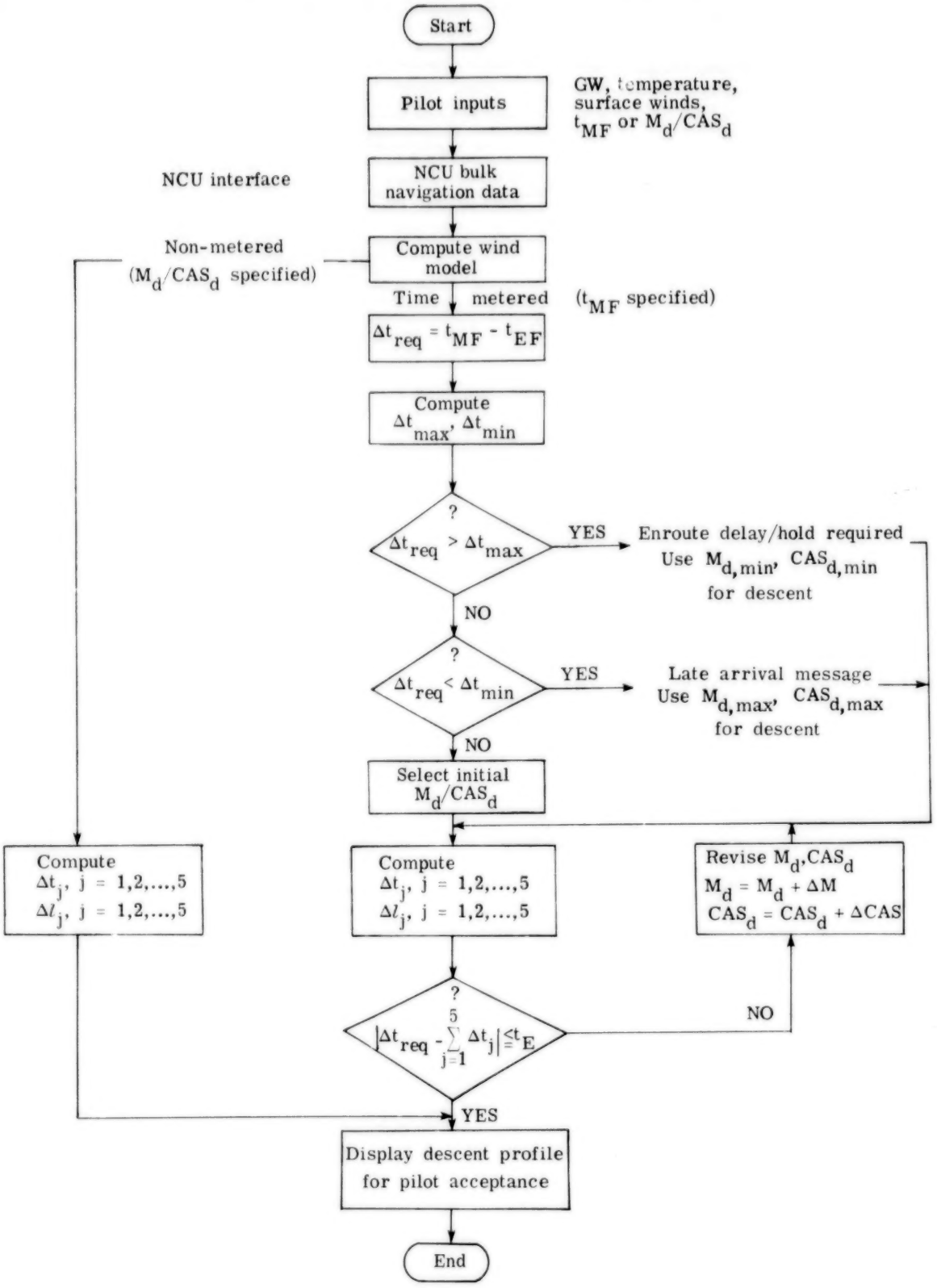
Start
Pilot inputs
GW, temperature, surface winds, t_{MF} or M_d/CAS_d
NCU interface
NCU bulk navigation data
Non-metered (M_d/CAS_d specified)
Compute wind model
Time metered (t_{MF} specified)
$\Delta t_{req} = t_{MF} - t_{EF}$
Compute Δt_{max}, Δt_{min}
? $\Delta t_{req} > \Delta t_{max}$
YES
Enroute delay/hold required
Use $M_{d,min}$, $CAS_{d,min}$ for descent
NO
? $\Delta t_{req} < \Delta t_{min}$
YES
Late arrival message
Use $M_{d,max}$, $CAS_{d,max}$ for descent
NO
Select initial M_d/CAS_d
Compute Δt_j, j = 1,2,...,5 $\Delta \ell_j$, j = 1,2,...,5
Compute Δt_j, j = 1,2,...,5 $\Delta \ell_j$, j = 1,2,...,5
Revise M_d, CAS_d
$M_d = M_d + \Delta M$
$CAS_d = CAS_d + \Delta CAS$
? $\left|\Delta t_{req} - \sum_{j=1}^{5} \Delta t_j\right| \leq t_E$
NO
YES
Display descent profile for pilot acceptance
End

Figure 2.- LFM/PD algorithm logic flow.

BLANK
PAGES

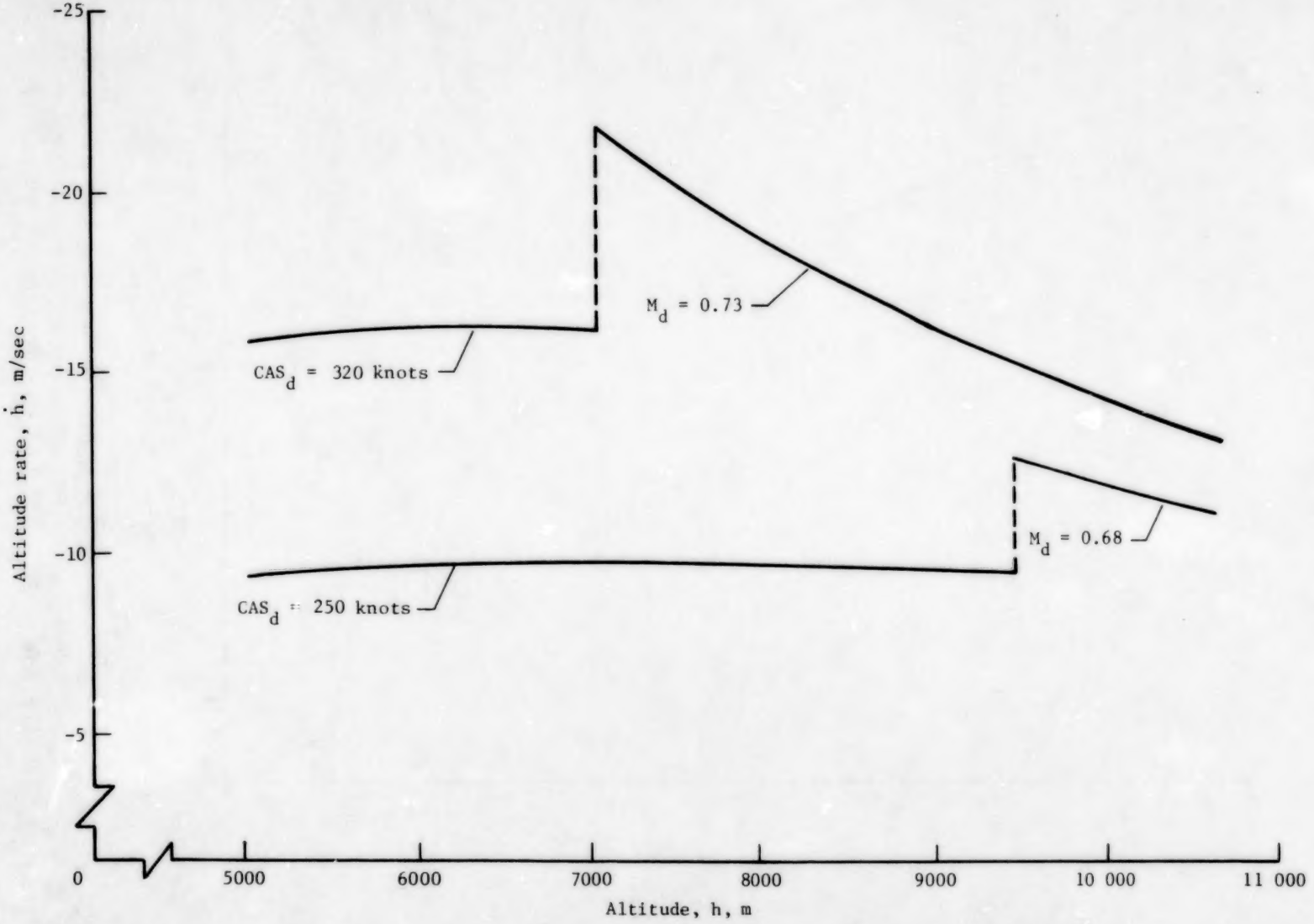

Figure 3.- Altitude rate flight performance data from initial altitude of 10 700 m for TCV Boeing 737 airplane. GW = 378 080 N; idle thrust (P&W JT8D-7).

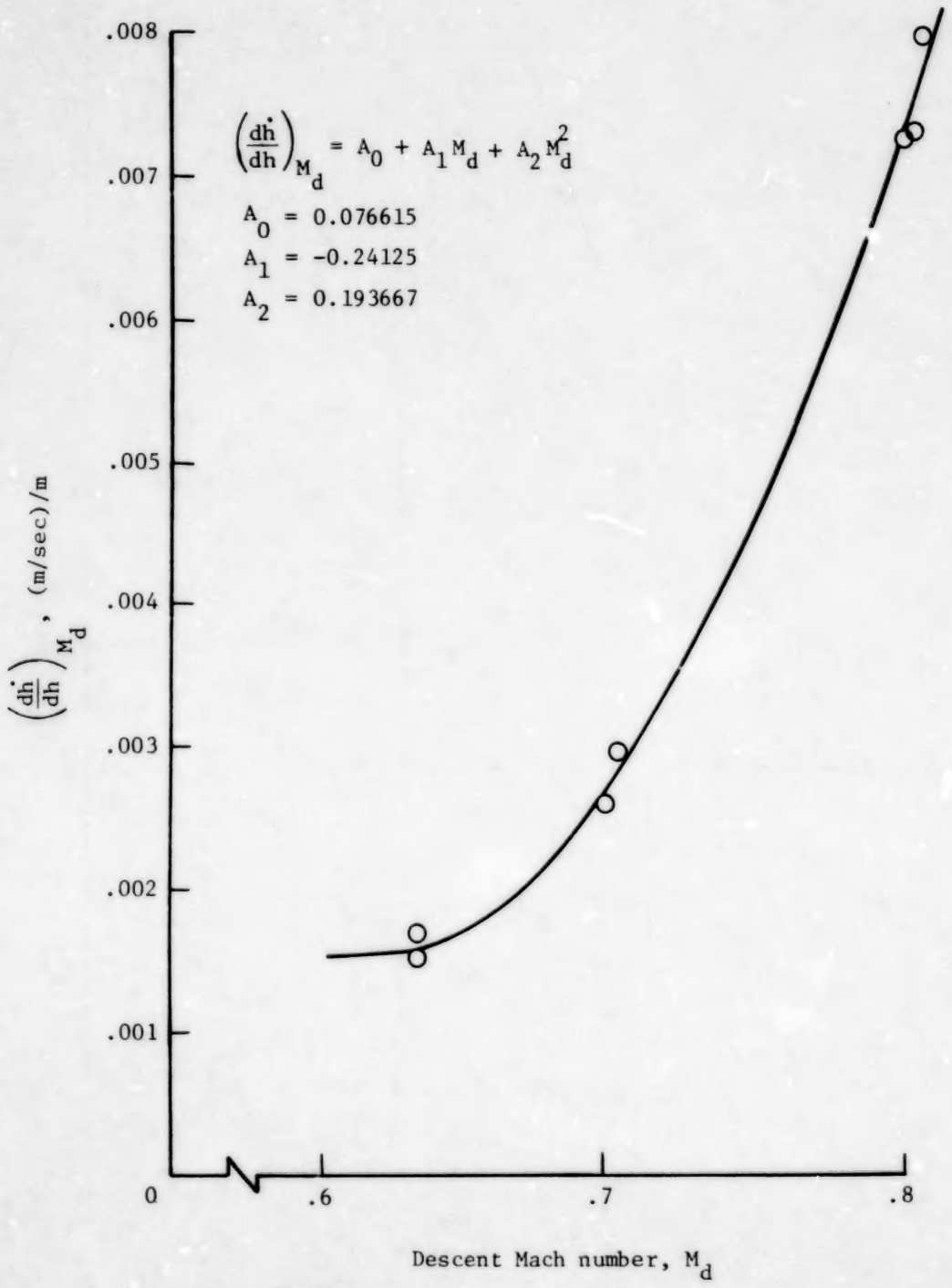

Figure 4.- Variation of $\left(\frac{\dot{dh}}{dh}\right)_{M_d}$ as a function of the descent Mach number for TCV Boeing 737 airplane. GW = 378 080 N; idle thrust (P&W JT8D-7).

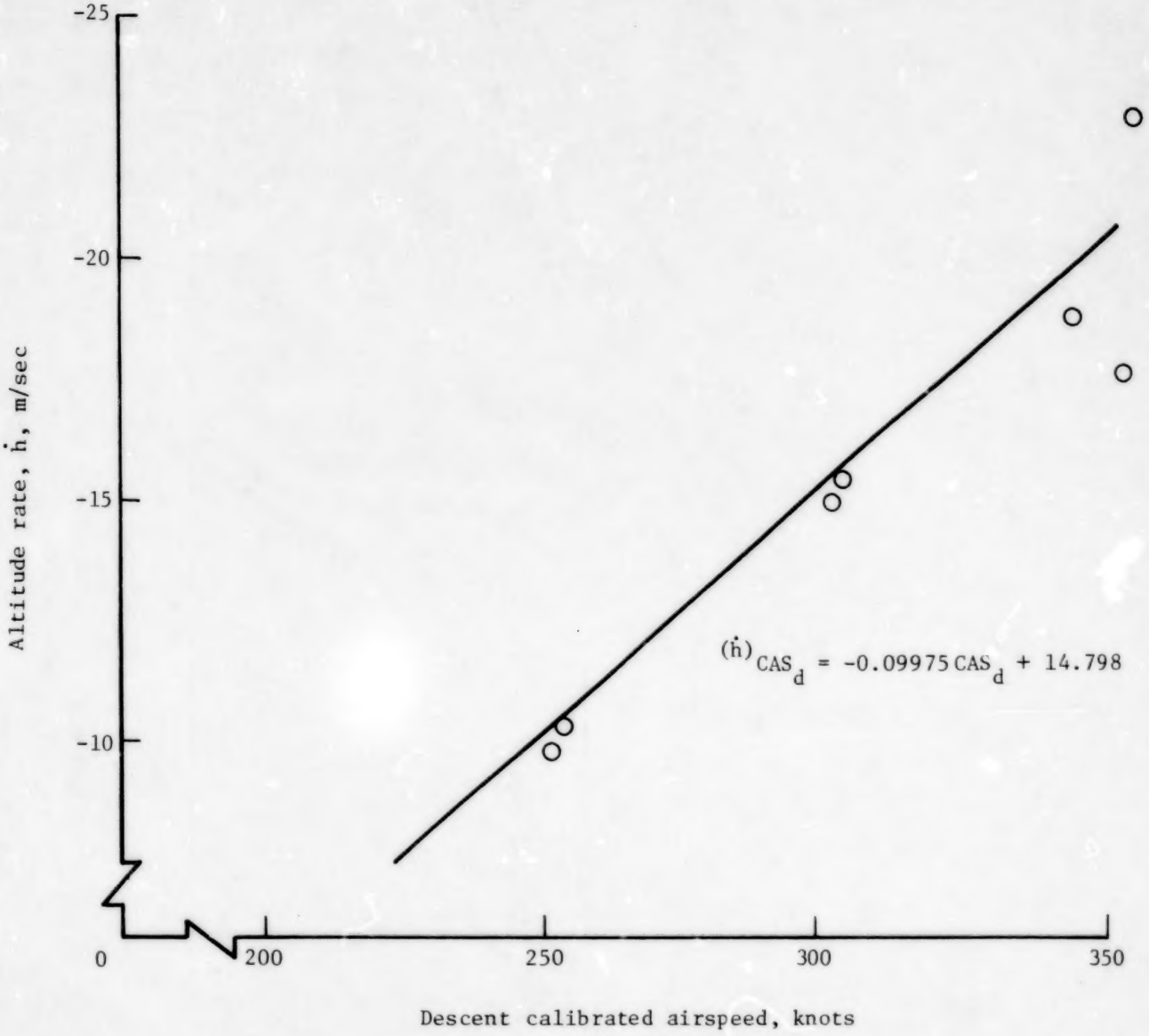

Figure 5.- Variation of altitude rate and descent CAS flight performance data for TCV Boeing 737 airplane. GW = 378 080 N; idle thrust (P&W JT8D-7).

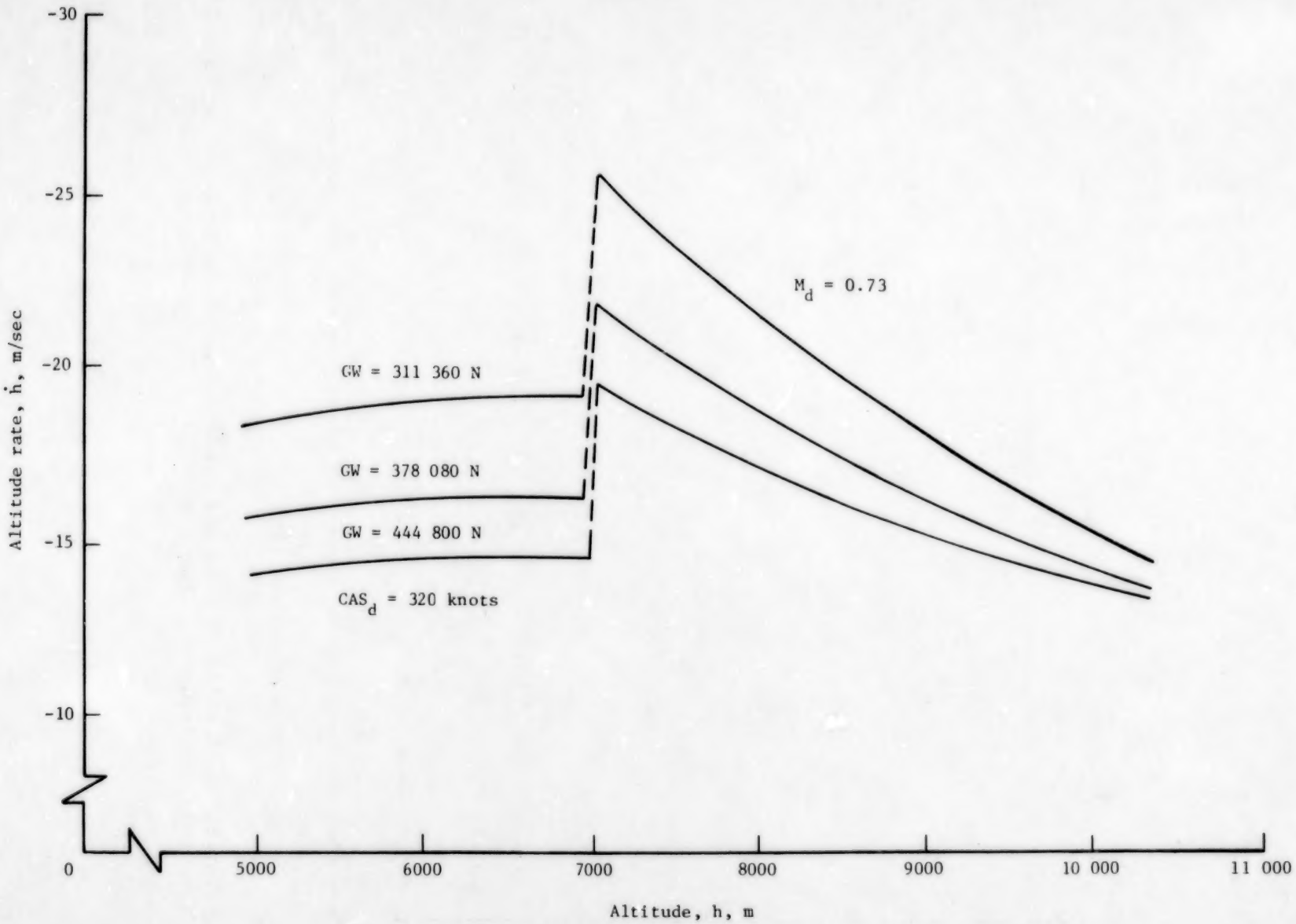

Figure 6.- Boeing 737 airplane simulation data for effects of gross weight on rate of descent. Idle thrust (P&W JT8D-7).

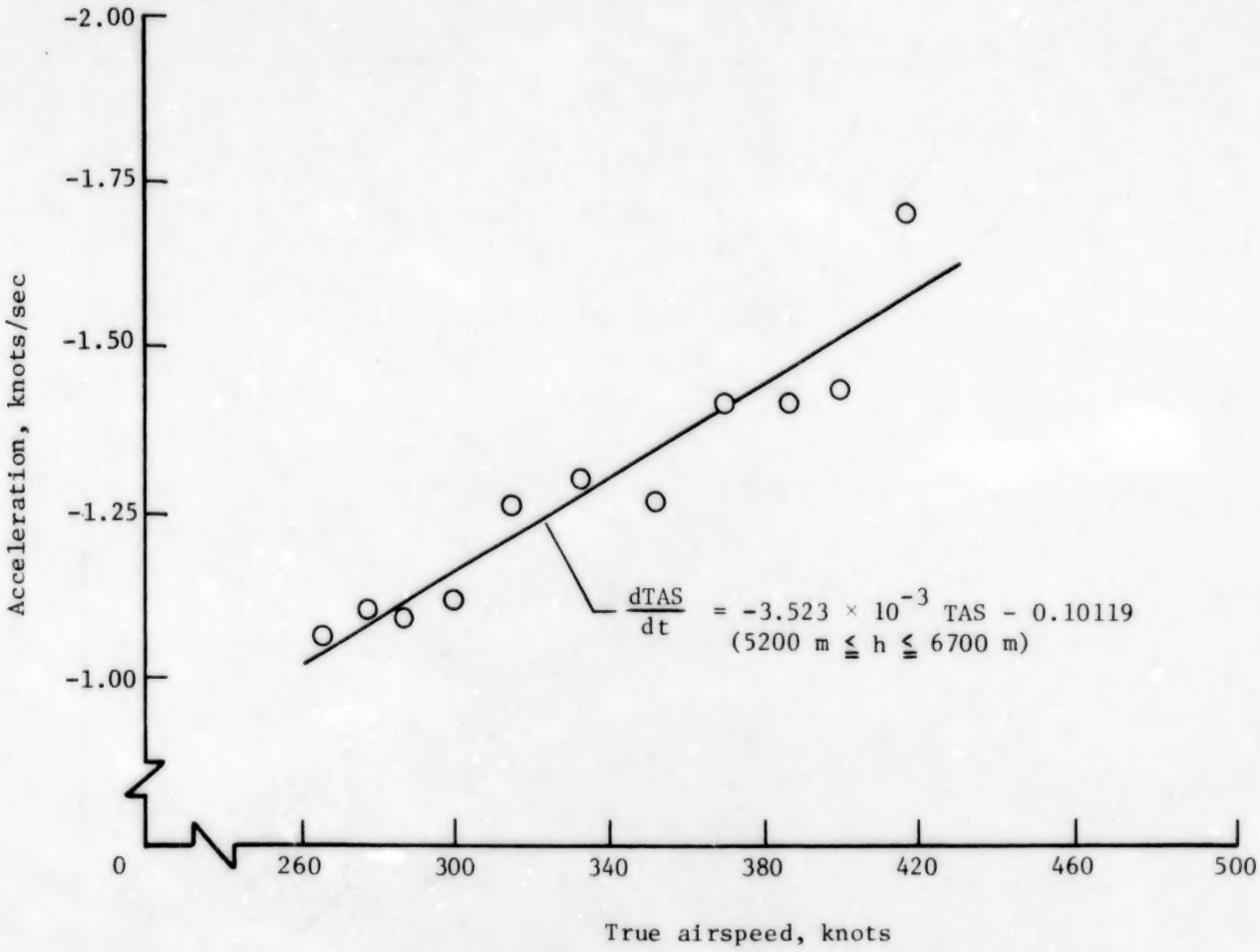

Figure 7.- Acceleration flight performance data for TCV Boeing 737 airplane.

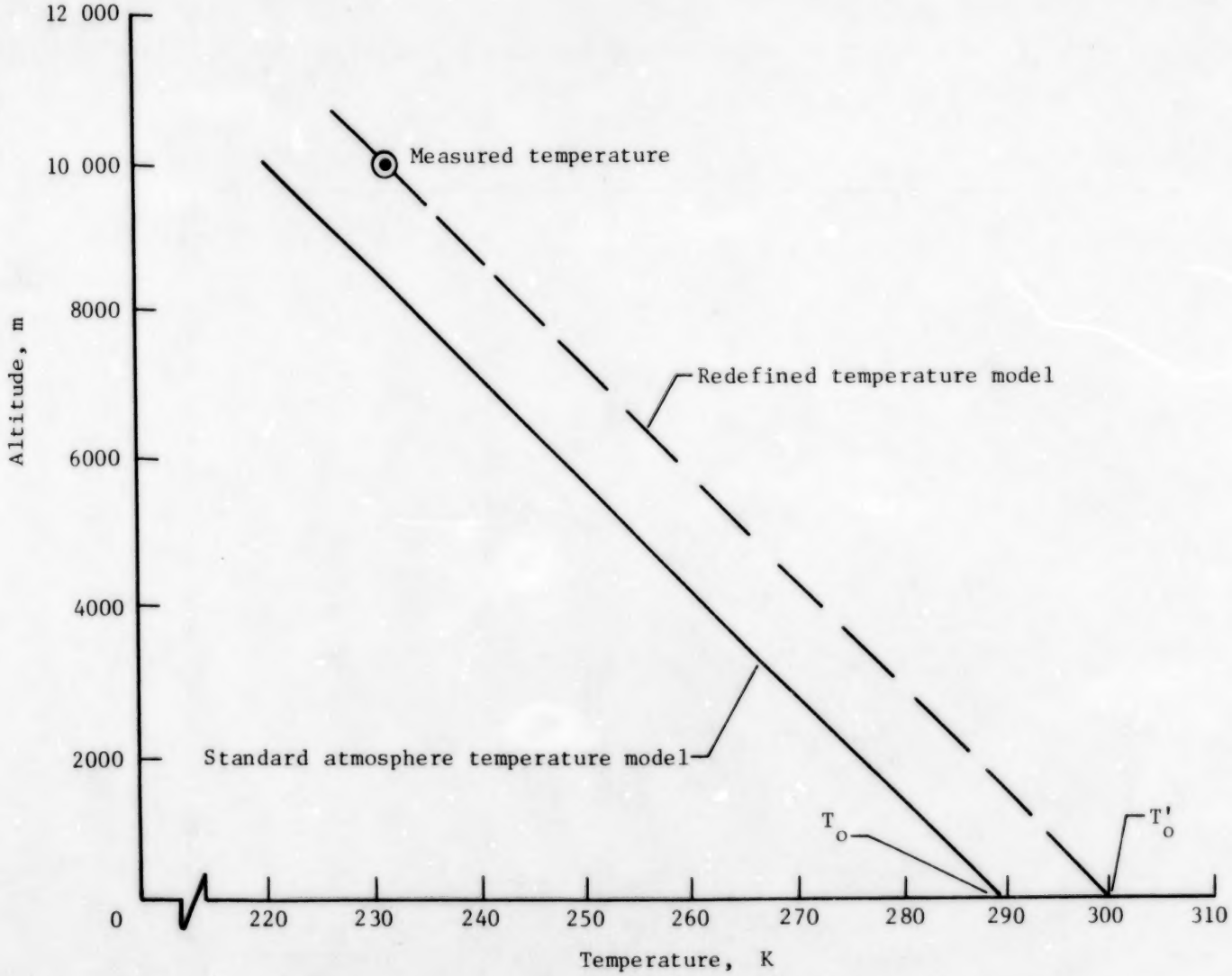

Figure 8.- LFM/PD algorithm temperature compensation.

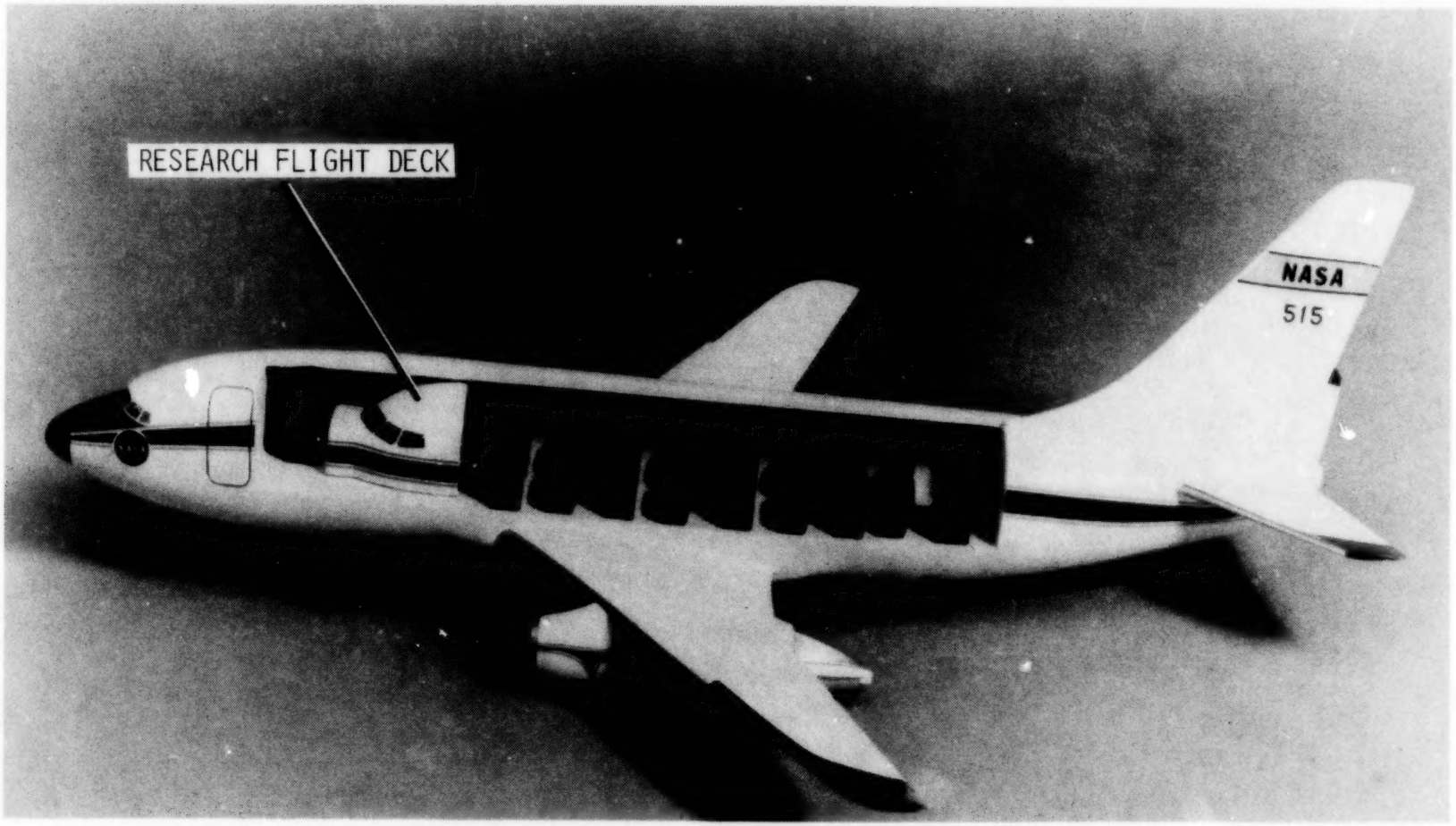

L-80-2578.1

Figure 9.- Cutaway view of TCV airplane.

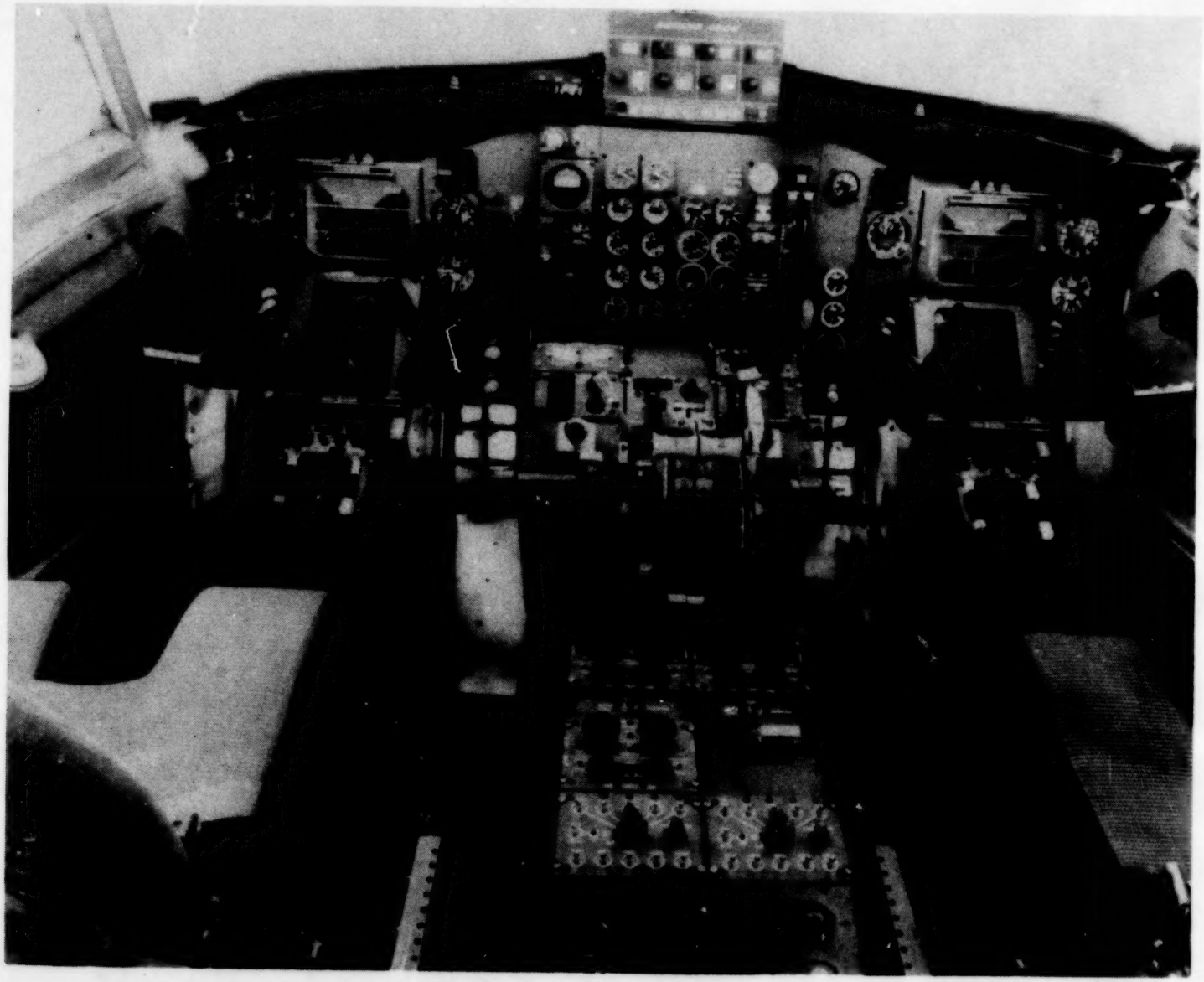

L-80-2514

Figure 10.- Instrument panel of research flight deck.

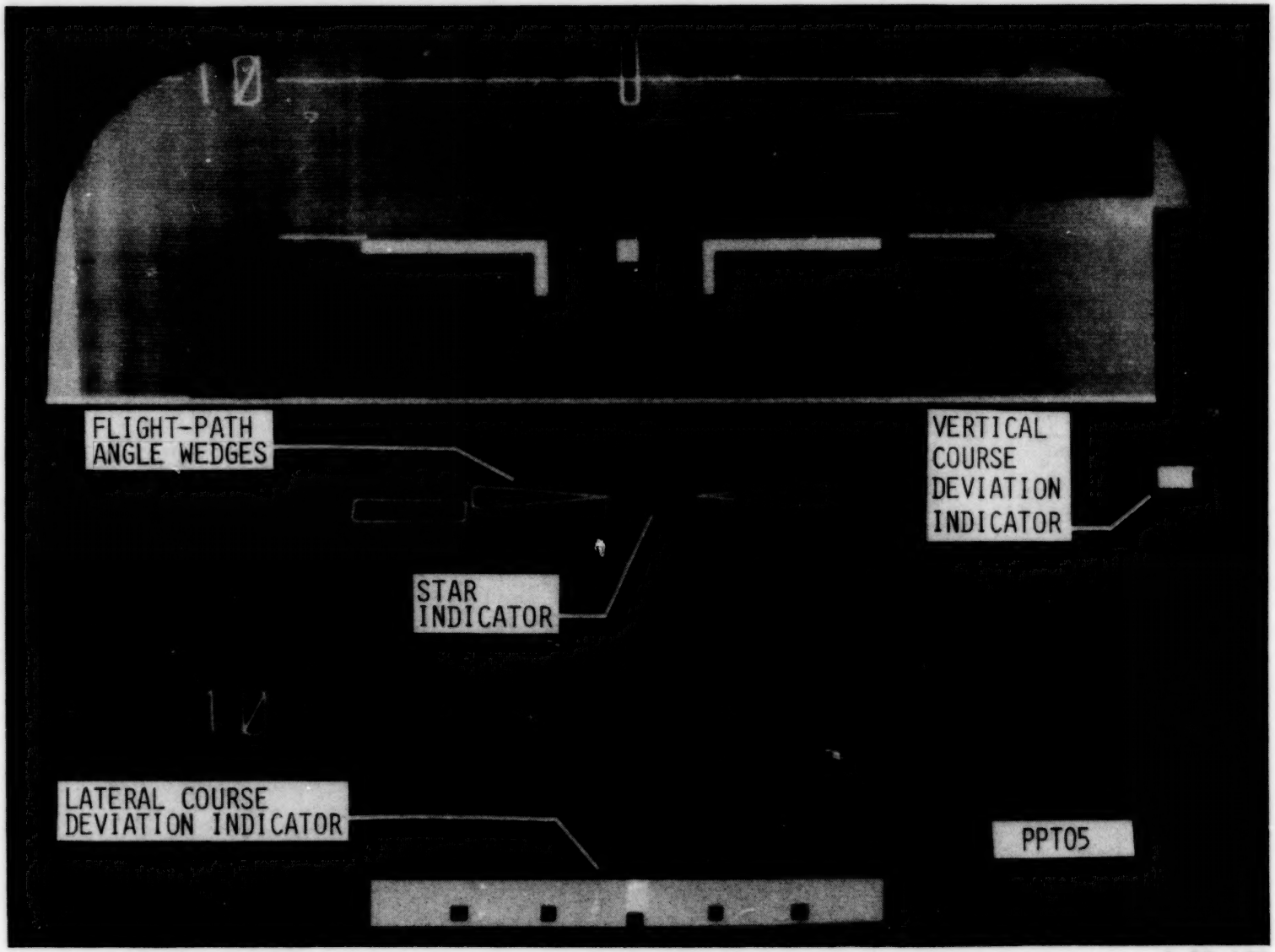

L-80-195

Figure 11.- EADI display with the course deviation indicators and the star and wedges guidance symbology.

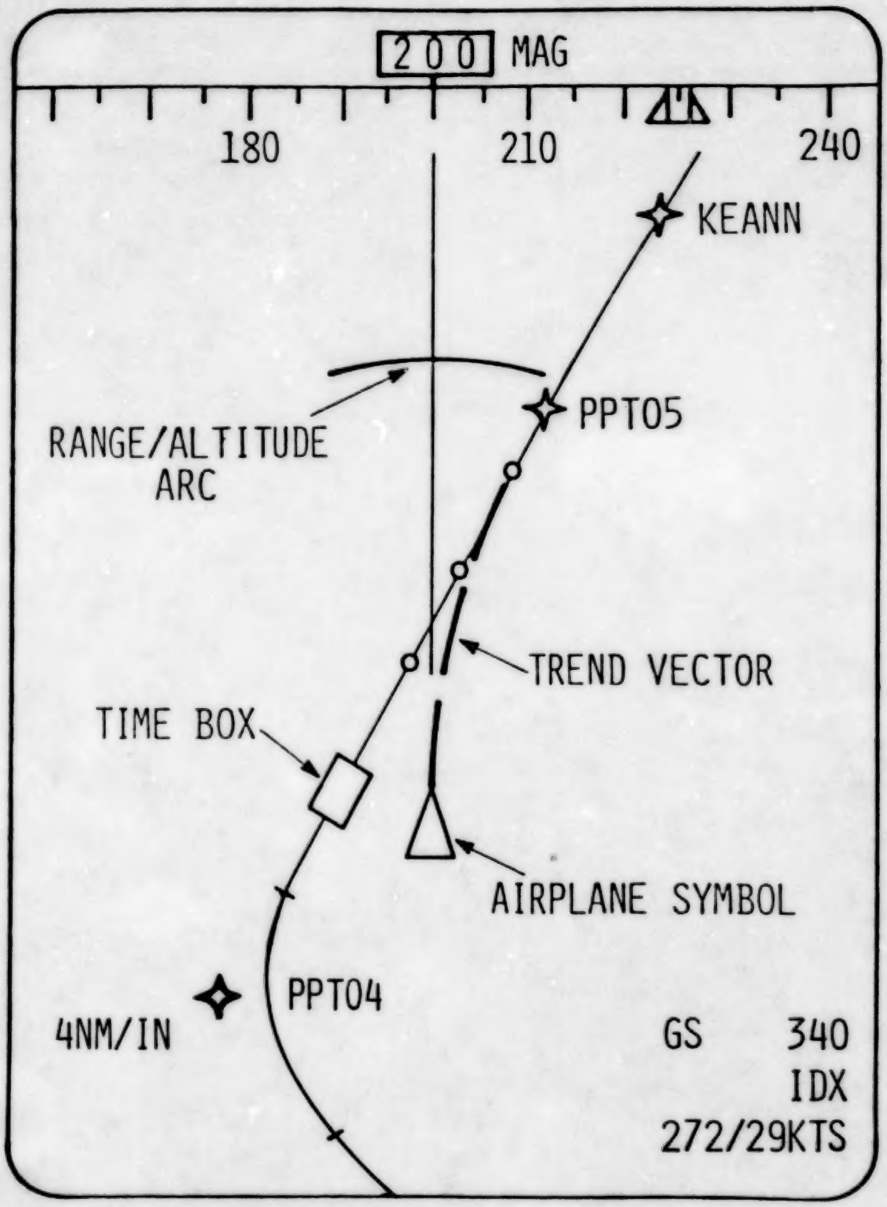

Figure 12.- EHSI display with the trend vector, range/altitude arc, and time guidance symbology. (1 in. = 2.54 cm.)

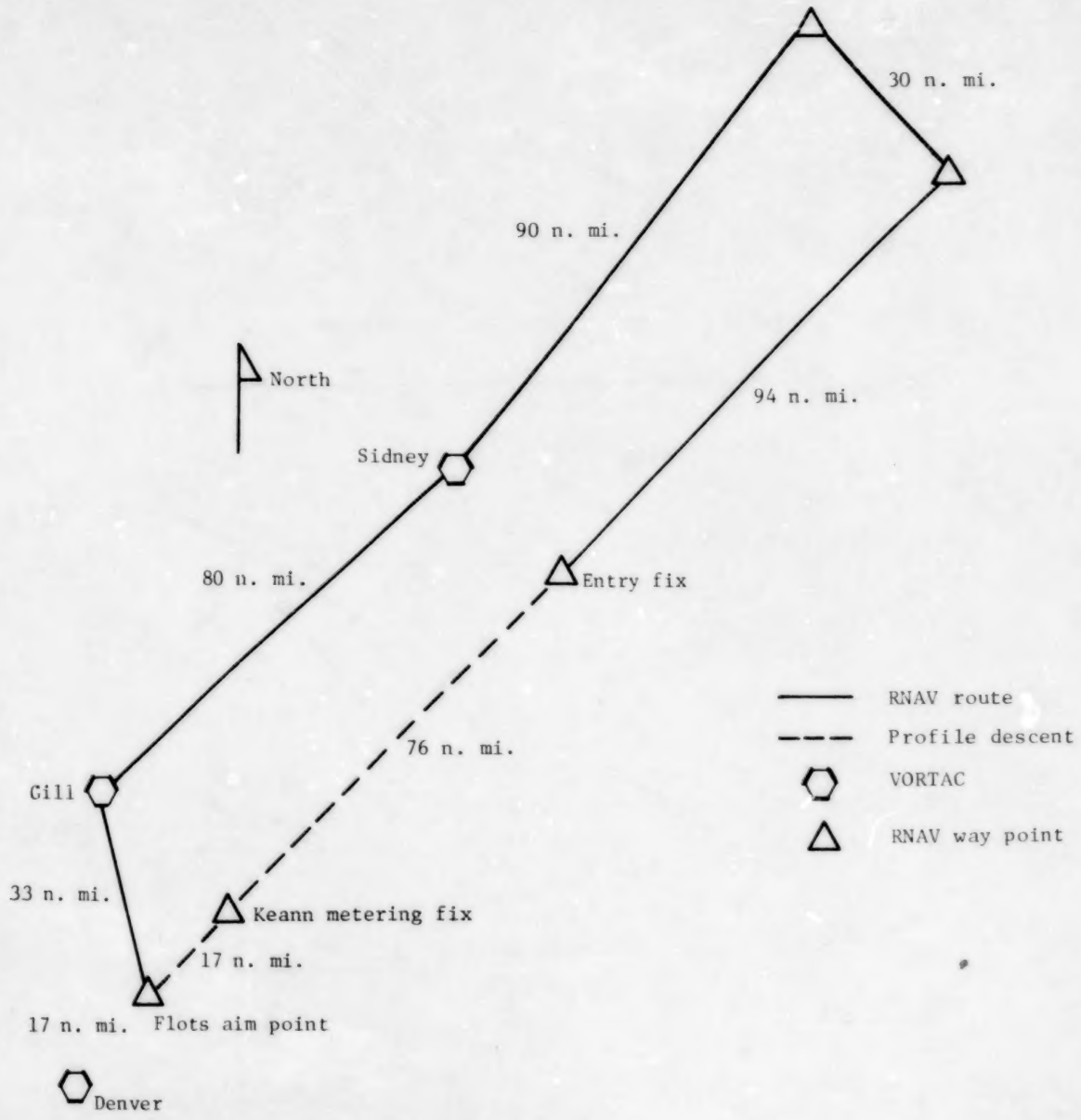

Figure 13.- LFM/PD flight test path.

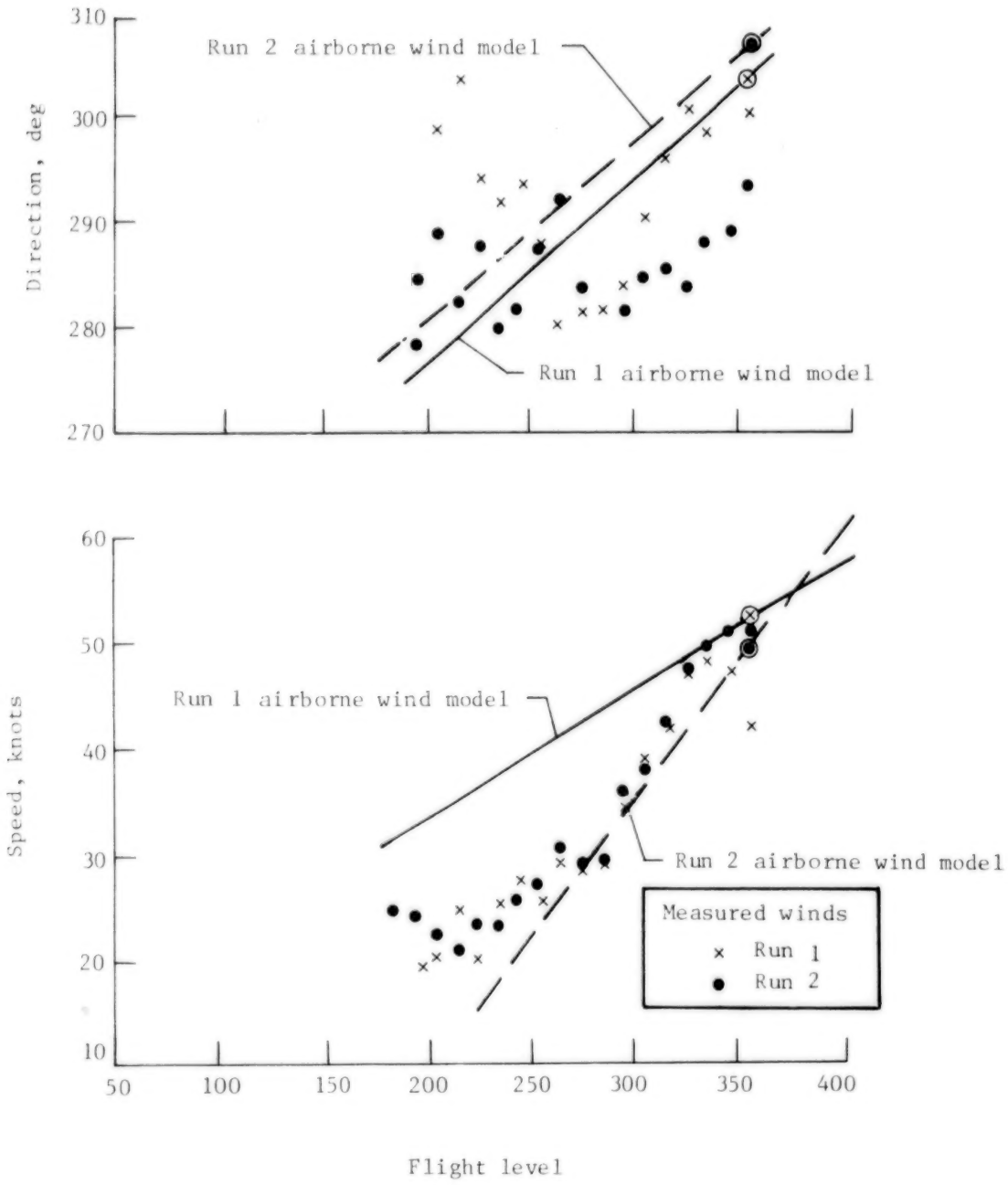

Figure 14.- Modeled and measured wind speed and direction (relative to magnetic north) for two runs. Circled data points are inertially measured speed and direction.

BLANK
PAGES

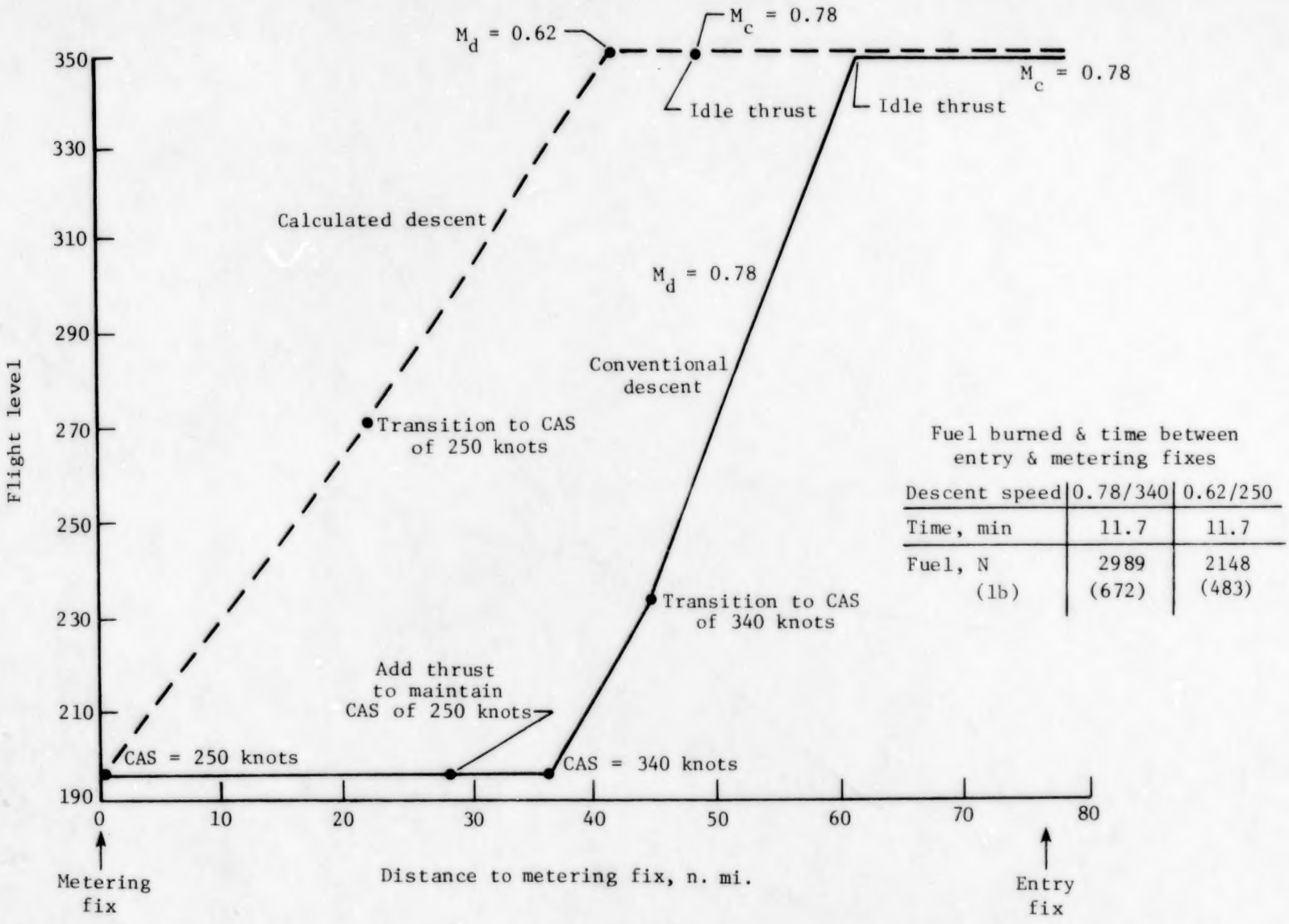

Fuel burned & time between entry & metering fixes

Descent speed	0.78/340	0.62/250
Time, min	11.7	11.7
Fuel, N (lb)	2989 (672)	2148 (483)

Figure 15.- Comparison of descent profile typically flown and descent profile calculated by flight management descent algorithm.

1. Report No.	2. Government Accession No.	3. Recipient's Catalog No.
NASA TP-1717		

4. Title and Subtitle	5. Report Date
DEVELOPMENT AND TEST RESULTS OF A FLIGHT MANAGEMENT ALGORITHM FOR FUEL-CONSERVATIVE DESCENTS IN A TIME-BASED METERED TRAFFIC ENVIRONMENT	October 1980
	6. Performing Organization Code
7. Author(s)	8. Performing Organization Report No.
Charles E. Knox and Dennis G. Cannon	L-13725
	10. Work Unit No.
9. Performing Organization Name and Address	534-04-13-52
NASA Langley Research Center Hampton, VA 23665	11. Contract or Grant No.
	13. Type of Report and Period Covered
12. Sponsoring Agency Name and Address	Technical Paper
National Aeronautics and Space Administration Washington, DC 20546	14. Sponsoring Agency Code

15. Supplementary Notes

Charles E. Knox: Langley Research Center.
Dennis G. Cannon: Boeing Commercial Airplane Company, Seattle, Washington.

16. Abstract

The NASA has developed and flight tested a simple flight management descent algorithm designed to improve the accuracy of delivering an airplane in a fuel-conservative manner to a metering fix at a time designated by air traffic control. This algorithm provides a three-dimensional path with terminal area time constraints (four-dimensional) for an airplane to make an idle-thrust, clean-configured (landing gear up, flaps zero, and speed brakes retracted) descent to arrive at the metering fix at a predetermined time, altitude, and airspeed. The descent path is calculated for a constant Mach/airspeed schedule from linear approximations of airplane performance with considerations given for gross weight, wind, and nonstandard pressure and temperature effects. This report describes the flight management descent algorithm and presents the results of the flight tests flown with the Terminal Configured Vehicle airplane.

17. Key Words (Suggested by Author(s))	18. Distribution Statement
Fuel conservation Flight management system Airplanes Air traffic control Airborne computer	Unclassified - Unlimited Subject Category 06

19. Security Classif. (of this report)	20. Security Classif. (of this page)	21. No. of Pages	22. Price
Unclassified	Unclassified	47	A03

For sale by the National Technical Information Service, Springfield, Virginia 22161

NASA-Langley, 1980

END

12/15/80